

# NET4mPLASTIC PROJECT

## WP4 - Activity 4.1 Monitoring plastic and microplastic wastes on coastal and marine environments

### D 4.1.2

Physical data (topography, bathymetry, temperature, salinity, etc.) and drone images

June 2022 – Final Version

<b>Project Acronym</b>	NET4mPLASTIC
<b>Project ID Number</b>	10046722
<b>Project Title</b>	New Technologies for macro and Microplastic Detection and Analysis in the Adriatic Basin
<b>Priority Axis</b>	3
<b>Specific objective</b>	3.3
<b>Work Package Number</b>	4
<b>Work Package Title</b>	Demonstration activities: testing and improvement of developed methodologies
<b>Activity Number</b>	4.1
<b>Activity Title</b>	Monitoring plastic and microplastic wastes on coastal and marine environments
<b>Partner in Charge</b>	LP – University of Ferrara (UNIFE)
<b>Partners involved</b>	LP – University of Ferrara (UNIFE) PP3 – Hydra Solution SRL PP5 – Veterinary Public Health Institute of Abruzzo and Molise Regions (IZSAM) PP6 – Teaching Institute for Public Health, Primorje-Gorski Kotar County (TIPH) PP7 – Department for EU Projects Planning and Implementation, Public Institution RERA S.D. for Coordination and Development of Split Dalmatia County (RERA) PP8 – University of Split - Faculty of Civil Engineering, Architecture And Geodesy (UNIST-FGAG)
<b>Status</b>	Final
<b>Distribution</b>	Public

<b>CONTRIBUTING PARTNERS</b>	UNIFE, HYDRA SOLUTION, TIPH, RERA, UNIST-FGAG
------------------------------	---

Data	Vers	Prep	Resp	Appr	Rev	Comment
28/02/2022	1.0	UNIFE	UNIFE	Vaccaro Carmela Corinne Corbau Elena Zambello Elisabetta Olivo Francesco Droghetti Umberto Tessari	Draft	Comment and approval
23/05/2022	1.1	UNIFE	UNIFE	Vaccaro Carmela Corinne Corbau Elisabetta Olivo Alberto Pellegrinelli Yuri Taddia	Draft	Comment and approval
31/05/2022	1.2	Rera (IOF)	UNIFE	Gorana Baničević Pero Tutman Dubravka Bojanić Varezić	Draft	Comment and approval
10/06/2022	1.3	FGAG	UNIFE	Roko Andricevic Toni Kekez	Draft	Comment and approval
15/06/2022	1.4	TIPH	UNIFE	Itana Bokan	Draft	Comment and approval
25/06/2022	1.5	Hydra Solution	UNIFE	Daniele Calore	Draft	Comment and approval
30/06/2022	1.6	WP4.1 partners	UNIFE	Vaccaro Carmela Corinne Corbau Elisabetta Olivo Joana Buoninsegni Maria Nicoli Francesco Droghetti Umberto Tessari	Final	Comment and approval

## INDEX

1	Introduction .....	5
2	Methods and Results .....	6
2.1	Topography / Bathymetry.....	6
2.1.1	Topo-bathymetric data acquisition and elaboration .....	6
2.1.2	Goro survey – June 2019.....	6
2.1.3	Boccasette survey – January 2020 .....	8
2.2	Physical properties measurements.....	11
2.2.1	Test site 1 and 2: Po Delta and Pescara area (IT).....	11
2.2.2	Test site 3: Rijeka area (HR) .....	26
2.2.3	Test site 4: Split area (HR).....	30
2.3	UAV OBU Marine drone campaign .....	39
2.3.1	Volano field campaign – October 2021 (Po Delta).....	41
2.3.2	Rijeka field campaign – October 2021 (Rijeka area) .....	42
2.3.3	Split field campaign – October 2021 (Split area) .....	44
2.3.4	Rijeka field campaign – May 2022 (Rijeka area) .....	46
2.3.5	Goro field campaign – May 2022 (Po Delta).....	47
2.4	Aerial Drone Imagery .....	48
2.4.1	Drone images data acquisition and elaboration.....	49
2.4.2	GIS elaboration and statistical analyses.....	54
3	References .....	57

## 1 Introduction

The river's mouth, lagoon beach and coastal waters of the Adriatic areas have been documented as hotspots of plastic pollution, due to the high density of the population living along rivers and coastal areas. In order to assess the risks of pollution derived from plastic diffusion, within NET4mPLASTIC Project a characterization activity was performed through the development of innovative methodologies, including the new sensors to be used with aerial and aquatic drones (see also WP4 and WP5 deliverables). The results reported below include also the redaction of protocols allowing the transferability of survey methods in highly sensitive ecosystems, which may become even more vulnerable when exposed to the negative impact of human activities.

In the context of the Work Package 4 of NET4mPLASTIC Project, the monitoring of the presence of micro and macroplastic on coastal and marine environments have been integrated with the collection of physical properties data, as well as topographic and bathymetric data. Innovative system, such as aerial and marine drone, has been tested to collect and elaborate images of the coastal area, in order to implement innovative methodologies for litter detection.

All these information has been collected in several locations within the 4 pilot sites (Po Delta, Pescara area, Rijeka and Split areas), whose main characteristics have been described in D.4.1.1.

## 2 Methods and Results

### 2.1 Topography / Bathymetry

As attested by scientific literature, periodic surveys were frequently carried out to verify the structural changes of the lagoon/coastal topography, and also in order to monitor the environmental qualities of seashore area, dunes evolution and shellfish farming.

Topographic/bathymetric campaigns were performed by University of Ferrara to improve the knowledge on the investigated area in the framework of the monitoring of marine litter in the coastal and marine area. Photogrammetric surveys (aerial drone) have been performed, in certain cases contextually with the topo/bathymetric ones, and are described in detail in this document in 2.4: Aerial Drone Imagery.

The topographic/bathymetric surveys were employed also to understand the causes and the impacts of pollution and its spread, and to reconstruct how specific changes in the bathymetry could modify the “normal” functionality of the ecosystem. These studies implemented in the Net4mPLASTIC project helped designing a model of the hydrodynamic transport and deposition of plastic in one of the Project test site (Po Delta area). The methodology and results of the model and related numerical simulation are described in WP3 deliverables. The numerical simulations allowed to develop an Early Warning System (EWS), described in detail in WP5 deliverables and published in the NET4mPLASTIC Project Web platform (<https://www.net4mplastic.com/>).

#### 2.1.1 Topo-bathymetric data acquisition and elaboration

During the first two years of the NET4mPLASTIC project, two topo/bathymetric surveys were carried out in the Po Delta area, in particular the first was carried out in summer 2019 (June 2019) in Goro (Ferrara), while the second in winter 2020 (January 2020) in Boccasette (Porto Tolle, Rovigo).

The main methodologies used for data acquisition are described below.

#### 2.1.2 Goro survey – June 2019

The reference system used for map restitution is that used by the Emilia Romagna Region European Datum 1950 - UTM 32 North (False Northing 4,000,000). The **topographical survey** has been carried out by detecting the planimetric position of the waterline through the acquisition of points approximately every 2 m. All positioning operations are performed with the GPS (Global Positioning System) differential mode RTK (Real Time Kinematics) model TRIMBLE 5700 (Master) 5800 (Rover). This system consists of two GPS receivers in dual frequency (L1/L2) and in communication with each other through the GSM network to minimize the positioning error. The receiver, defined base, is placed on a known point (cornerstone). Once the reception is calibrated, the instrument is able to verify the error in positioning X, Y, Z coordinates to which it is subject instant by instant. Through data transmission via GSM

this error is transmitted in real time to the other GPS receiver, called rover, which can then record already correct measurements.

The system allows to obtain topographic measurements with a millimetric precision, depending on: the distance between the base and the rover; the accuracy of the operator; the local calibration for the transformation from the GPS source coordinates (Lat. Long. in WGS 84 format) to the reference grid. Using this acquisition system, the maximum average error in the measurement of the profile points can be evaluated in about 2 cm in plan and 5 cm in altitude. Given the purpose of the surveys and the characteristics of the territory in question, this tolerance can be considered to be largely adequate.

For the **bathymetric survey**, in addition to the X Y Z positioning made with the same instrumentation of the topographic one, it is necessary to know the depth of the water. For this purpose, a single-beam hydrographic single-frequency depth echo-sounder has been used that allows centimetric precisions if suitably calibrated. Considering to the investigated depths (about -1/-6 m) the accuracy is about 2.5 cm. Therefore, the GPS receiver, in communication with the base positioned on the cornerstone, exactly as for the reliefs on the ground, is placed at the upper end of a rod made integral with the boat, while the transducer of the echo sounder is placed at the lower end, under the free surface of the water. The information provided by the two instruments (positioning from the GPS, including the length of the rod, and the measurement of the water column under the transducer coming from the echo sounder) are associated by a special navigation program (Navigator Professional) which records the data thus composed at a frequency of 1 Hz. During the data acquisition, the ellipsoidal dimensions provided by the GPS are recorded, which, during the processing phase, are transformed into geodetic quotas by applying a local geoid called GOROGEO 2005. This relatively complex data acquisition technique offers the chance of accurately following previously established navigation routes and not having to compensate the bathymetric measurements with the tidal value, which it is not always possible to establish with sufficient precision. In fact, the measurements, being related to the ellipsoid, do not express the measure of the depth of the water, but, with an algebraic operation, the operator can reach the actual depth of the bottom with the difference in level between the latter and zero.

The topographical and bathymetric survey and sampling, performed within the duration of the project, was carried out along transects perpendicular to the shoreline, which extended from the beach towards sea for 6 m.

The data were processed and then imported into the GIS environment in order to reconstruct by interpolation of the points detected the isobates every 0.25 m (*Figure 1*).

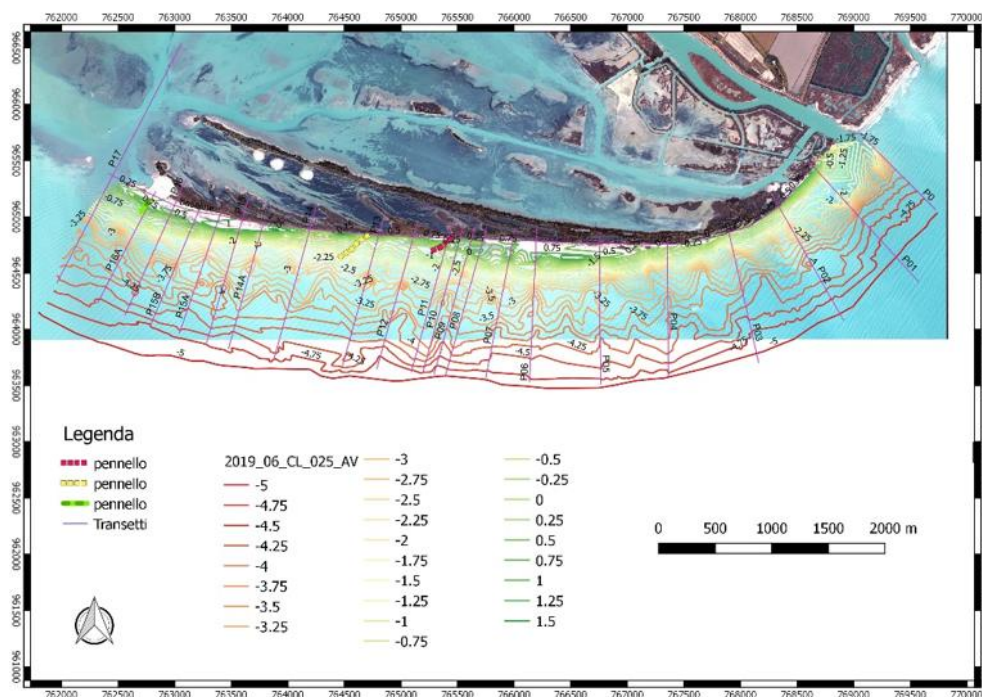


Figure 1: Map of the bathymetric survey of June 2019 performed on Goro beach.

### 2.1.3 Boccasette survey – January 2020

The **bathymetric survey** was carried out on some channels inside the lagoon, on the sea outlets and on the submerged beach in front of the Scanno di Goro along about 30 transects, at depths averagely between - 0.8 m and - 6 m. In continuity with the bathymetric profiles, the topographic survey was carried out on the beach. The activities were always carried out in conditions of calm sea, weak wind and no rainfall. The transects have been realized towards the sea up to the bathymetric -6 meters, equal to an average distance from the shore of about 1000 meters (*Figure 2*).

The surveys have been conducted by a lagoon boat on which the following instrumentation was installed: a single-beam hydrographic single-frequency depth echo-sounder; a R8 Trimble dual frequency GNSS geodetic receiver connected to a base receiver positioned on the Regional cornerstone VTR0068\_73\_07; the NavPro software produced by Communication Technologies, used for instrument interfacing, NMEA string coupling, latency management, data acquisition and navigation.

At the beginning and at the end of the survey activities, a calibration of the echo sounder was carried out through a "Bar-Check" procedure that involves the use of a metal plate lowered into the water below the transducer, in order to verify the correct reading of the depth by the echo sounder, and possibly change the speed of the sound in the water. The acquired data were first fixed by correcting the sporadic points where the quality of the GPS data was not of type "FIX", and then filtered and purified by the "false echo" bathymetric (through QGIS software).



The **topographic survey** was carried out with the main objective of characterizing the geomorphology of the emerged beach. The coordinates were acquired through the use of 1 dual-frequency GNSS (Global Navigation Satellite System) receiver (L1 and L2) Hiper-SR model of the manufacturer Topcon in NRTK mode (Network Real Time Kinematic) through the connection to the network of permanent NETGEO stations framed in the reference system ETRF2000-(2008).

The topography was performed on several days at low tide. The data was managed through the topographic software Mercury version 2015. In continuity with the bathymetric profiles, the coordinates X, Y, Z of about 800 points were acquired along 29 orthogonal profiles at the coast spaced 500 meters along the dune system (*Figure 2*) (*Figure 3*).

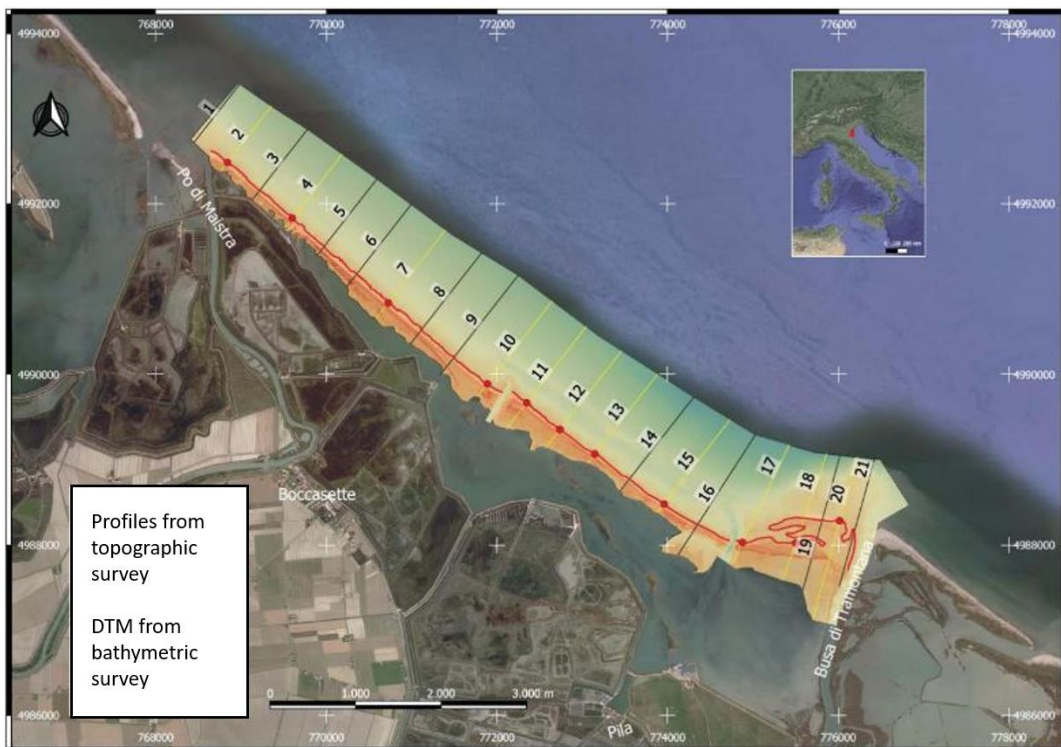


*Figure 2: Topo-bathymetric profiles and digital model of the seabed in Boccasette area.*

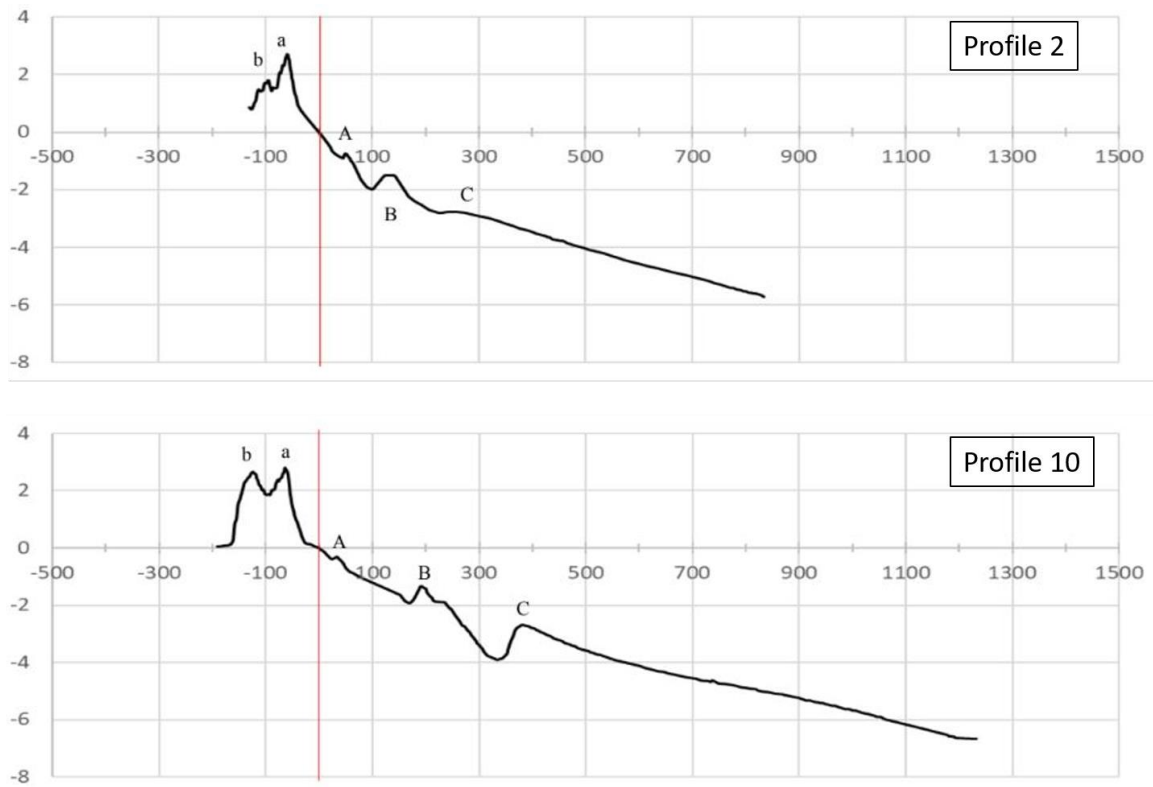


Figure 3: Examples of topographic profiles acquired in Boccasette (positioning in previous Figure).

## 2.2 Physical properties measurements

Physical properties measurements (T°, salinity, transparency, dissolved ox, pH, pressure depth, etc.) have been performed in all Project pilot sites, but as stated for the other sampling campaigns (D.4.1.1 and the previous chapter in this deliverable), not at the same time and in all the locations. In this chapter the main procedures of physical properties measurements are described, as well as the results obtained, and some comparison with already existing data from regional and national research associations.

The methods used for physical measurements are standardised ISO methods, except for the transparency of sea water which is measured in situ by using a Secchi disk (*Table 1*). The depth where the Secchi disk settles beyond visual recognition is called *Secchi depth* and it is an index of water transparency. The disk is slowly lowered until its visibility is compromised and then raised until it just reappears at the observer. The average of the two measurements represents the Secchi disk visibility index.

*Table 1: Methods used in physical properties measurement.*

Physico-chemical indicators	Method
<i>Temperature (1°C to 90°C)</i>	Standard Methods for the Examination of Water and Wastewater 23 <sup>rd</sup> Ed. 2017. 2550 B*, APHA, AWWA, WEF. Determination of temperature.
<i>pH</i>	HRN EN ISO 10523:2012, Determination of pH (ISO 10523:2008; EN ISO 10523:2012). ISO 10523:2008 specifies a method for determining the pH value in rain, drinking and mineral waters, bathing waters, surface and ground waters, as well as municipal and industrial waste waters, and liquid sludge, within the range pH 2 to pH 12 with an ionic strength below $I = 0,3 \text{ mol/kg}$ (conductivity at 25 °C < 2 000 mS/m) solvent and in the temperature range 0 °C to 50 °
<i>Dissolved oxygen</i>	Intellical LDO101, Hach Lange, digital probe, luminescent dissolved oxygen probe measures the dissolved oxygen concentration in wastewater, drinking water and general water samples. The probe has temperature and absolute air pressure sensors for accurate dissolved oxygen measurements.
<i>Salinity–conductometry</i>	Standard Methods for the Examination of Water and Wastewater 23 <sup>rd</sup> Ed. 2017. 2520 B. APHA, AWWA, WEF. Determination of salinity.
<i>Transparency of sea water</i>	Transparency is measured in situ by using a Secchi disk.

### 2.2.1 Test site 1 and 2: Po Delta and Pescara area (IT)

Physical properties data have been investigated in both of the Italian test site, Po Delta and Pescara area in the last two years of the Project.

In the first Pilot site measurements have been taken in autumn 2021 (October 2021), in three different locations (Rosolina, Boccasette and Goro), as listed in *Table 2*. In this case the sampling has been realized at two depths (-0,1m and -4m). Physical properties data are shown in *Table 3*.

Table 2: Physical-chemical indicators of sea water measured during microplastics sampling in Po Delta Areas.

Sample ID	Sampling Date	Time	Sampling Site	Latitude Longitude	Depth (m)
2021_10_18_Ros_0.1	18/10/2021	12:13	Rosolina	45,113127 N 12,34917 E	-0,1
2021_10_18_Ros_4	18/10/2021	12:14	Rosolina	45,113127 N 12,34917 E	-4
2021_10_19_BBMCa_0.1	19/10/2021	11:22	Boccasette	45,041717 N 12,446322 E	-0,1
2021_10_19_BBMCa_4	19/10/2021	11:23	Boccasette	45,041717 N 12,446322 E	-4
2021_10_19_BBMCb_0.1	19/10/2021	13:45	Boccasette	45,034274 N 12,454187 E	-0,1
2021_10_19_BBMCb_4	19/10/2021	13:43	Boccasette	45,034274 N 12,454187 E	-4
2021_10_20_Goro_0.1	20/10/2021	11:14	Goro	45,759863 N 12,333317 E	-0,1
2021_10_20_Goro_4	20/10/2021	11:13	Goro	45,759863 N 12,333317 E	-4

Table 3: Dates and sampling locations of physical measurements obtained during sampling of microplastics in sea water surface in Delta Po Test Sites.

Sample ID	Depth (m)	°C	pH	OxRedPot	Conducibility mS/cm	Total Dissolved Solid ppm	Salinity	psi	atm
Ros_0.1	-0,1	16,99	8,26	32,4	50,14	30080	32,93	23,9	1,0129
Ros_4	-4	17,26	8,26	35,9	50,99	30590	33,56	24,3	1,0132
BBMCa_0.1	-0,1	15,88	8,25	47,4	44,95	26970	29,15	21,3	1,017
BBMCa_4	-4	15,82	8,25	47,9	44,9	26940	29,11	21,3	1,0171
BBMCb_0.1	-0,1	16,46	8,24	62,4	44,63	26780	28,92	21	1,0173
BBMCb_4	-4	16,64	8,24	59,9	47,48	28490	30,99	22,5	1,0175
Goro_0.1	-0,1	16,53	8,38	25,4	39,98	23990	25,61	18,4	1,0141
Goro_4	-4	18,05	8,29	23,2	50,22	30130	32,99	23,7	1,0141

In the second Pilot site measurements have been taken in spring 2021 (May 2021) and winter 2022 (February 2022), in one location (Montesilvano), as listed in *Table 4*. In this case the sampling has been realized at four depths (sea surface, -0,1m, -3m and -4m). Physical properties data are shown in *Table 5*.

*Table 4: Physical-chemical indicators of sea water measured during microplastics sampling in Pescara area.*

Sample ID	Sampling Date	Time	Sampling Site	Latitude Longitude	Depth (m)
P1	26/05/2021	16:42	Montesilvano	42.516985 N 14.168189 E	-3
P2	26/05/2021	16:44	Montesilvano	42.516555 N 14.167344 E	-3
P3	26/05/2021	16:46	Montesilvano	42.516495 N 14.167462 E	0
P4	26/05/2021	16:51	Montesilvano	42.517879 N 14.169563 E	-3
P5	26/05/2021	16:53	Montesilvano	42.517746 N 14.169287 E	0
Montesil A	09/02/2022	12:52	Montesilvano	42.519713 N 14.186417 E	-0,1
Montesil B	09/02/2022	12:53	Montesilvano	42.519713 N 14.186417 E	-4
Montesil C	09/02/2022	13:51	Montesilvano	42.516901 N 14.17401 E	-0,1
Montesil D	09/02/2022	13:53	Montesilvano	42.516901 N 14.17401 E	-4

*Table 5: Dates and sampling locations of physical measurements obtained during sampling of microplastics in sea water surface in Delta Pescara Test Sites.*

Sample ID	Depth (m)	°C	pH	OxRedPot	Conducibility mS/cm	Total Dissolved Solid ppm	Salinity	psi	atm
P1	-3	21,56	8,33	186,6	44,45	26670	28,77	14,8	-
P2	-3	21,56	8,33	192	44,46	26670	28,77	14,8	-
P3	0	22,17	8,31	195,5	43,98	26390	28,42	14,8	-
P4	-3	21,48	8,34	223,8	44,43	26660	28,75	14,8	-
P5	0	21,57	8,34	219,9	44,41	26650	28,74	14,8	-
Montesil A	-0,1	9,12	8,29	64,3	50,07	30040	32,61	-	1,0195
Montesil B	-4	9,05	8,28	63,4	49,93	29960	32,5	-	1,0195
Montesil C	-0,1	9,17	8,26	67,5	50,12	30070	32,65	-	1,0186
Montesil D	-4	8,84	8,28	66,2	50,12	30070	32,63	-	1,0186

### 2.2.1.1 Test site 1 and 2: comparison with existing data

The chemical-physical data of transitional water and seawater acquired by Net4mPlastic Project in the first two Pilot sites have been compared with the parameters acquired in the routine monitoring activities of ARPA (Italian regional agencies for the protection of the environment), through their monitoring stations.

The analyses performed by ARPA include the collection of samples taken with a Niskin bottle at 50 cm from the surface; a sample part is dedicated to the study of phytoplankton communities. Water samples for soluble nutrient determinations are filtered on site, using membrane filters with a porosity of 0.45  $\mu\text{m}$ ; the untouched samples and the filtered ones are then transported to the laboratory for subsequent analysis, kept in containers refrigerated at +4 °C. The sampling of marine sediment for the chemical-physical, biological, chemical and toxicological analyses, instead, is carried out through Van Veen grab sampler. The study of the benthic community is carried out by taking three replicas for each station, and sieving each sample of sediment through a sieve with a 1 mm mesh. The separated organisms are immediately fixed in a 70% + ethanol solution 5% glycerol in seawater and transported to the laboratory for classification.

The reference sites for the ARPA data and information are:

- <https://www.arpa.veneto.it/arpavinforma/bollettini/dati-in-tempo-reale/boe/index.php>  
(Veneto Region)
- <https://www.arpae.it/it/temi-ambientali/acqua/dati-acque/acque-di-transizione>  
(Emilia Romagna Region)
- [https://www.artaabruzzo.it/download/aree/acqua/acque\\_mc/20160325\\_AL\\_acque\\_marino\\_cost\\_aII\\_01.pdf](https://www.artaabruzzo.it/download/aree/acqua/acque_mc/20160325_AL_acque_marino_cost_aII_01.pdf)  
(Abruzzo Region)

The stations that were selected for the comparison of the monitored parameters are listed below (*Figure 4, Figure 5, Table 6, Table 7, Figure 6*). The selected ARPA stations are placed close to the NET4mPLASTIC sites (within Po Delta and Pescara area).

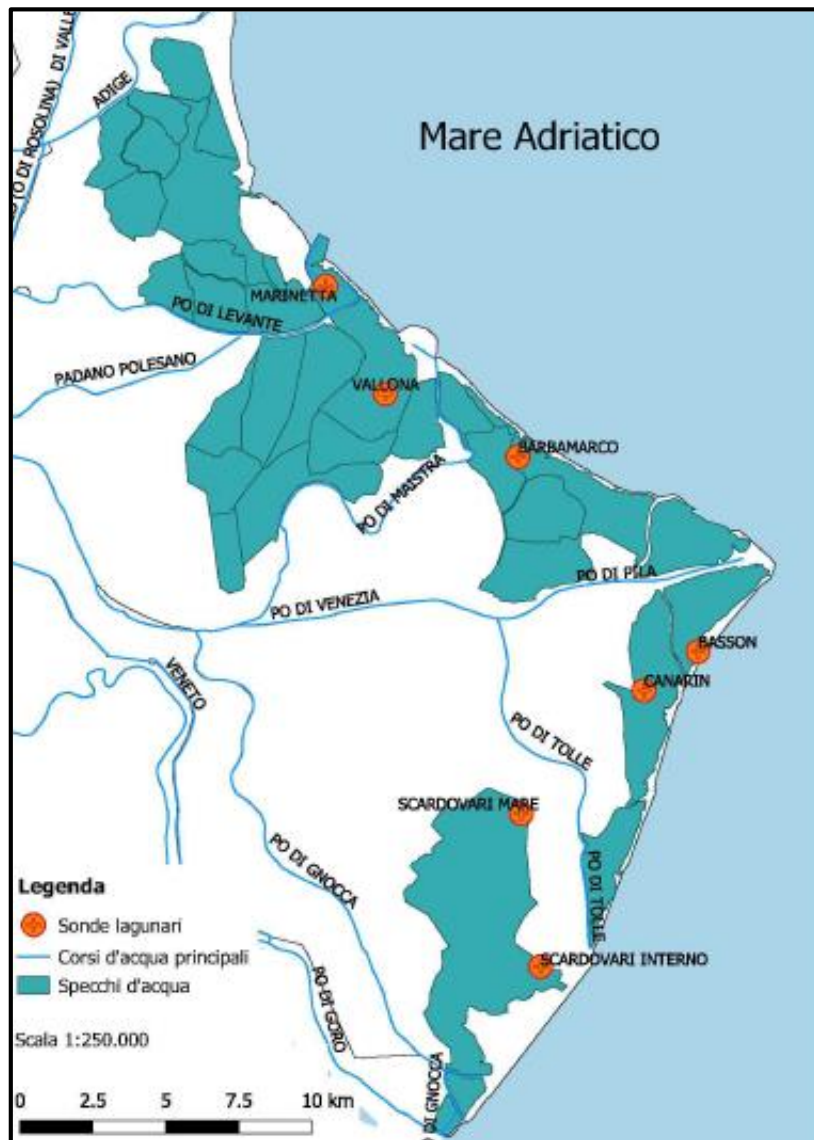


Figure 4: Localization of monitoring stations in the Veneto Network (ARPAV).



Figure 5: Localization of monitoring stations in the Emilia Romagna Network (ARPAE).

Table 6: Positioning of monitoring stations in the Emilia Romagna Network (ARPAE).

Water Body Name	Station Code WISE Code 2016	Acronym	Location	Longitude	Latitude
Sacca di Goro	99100401 IT0899100401	SGOR4bis	Bocca a mare Goro	Lat_ETRS89_32 4965365	Lon_ETRS89_32 762174
Sacca di Goro	99100100 IT0899100100	SGOR1	Foce Volano	Lat_ETRS89_32 4968448.266	Lon_ETRS89_32 759059.533
Sacca di Goro	99100201 IT0899100201	SGOR2bis	Gorino	Lat_ETRS89_32 4965650.696	Lon_ETRS89_32 765111.799
Sacca di Goro	99100300 IT0899100300	SGOR3	Porto Gorino	Lat_ETRS89_32 4968080.396	Lon_ETRS89_32 763327.194

Table 7: Positioning of monitoring stations in the Abruzzo Network (ARTA).

Water Body Name	Station Code Acronym	Longitude	Latitude	Depth (m)
PINETO 300 m south of the Vomano river	PI16	42 ° 39'14"	14 ° 02'43"	4,5
	PI18	42°39'45"	14°04'24"	12,0
PESCARA area in front of Cadorna Street	PE04	42°29'18"	14°12'06"	5,6
	PE06	42°30'04"	14°13'37"	14,4



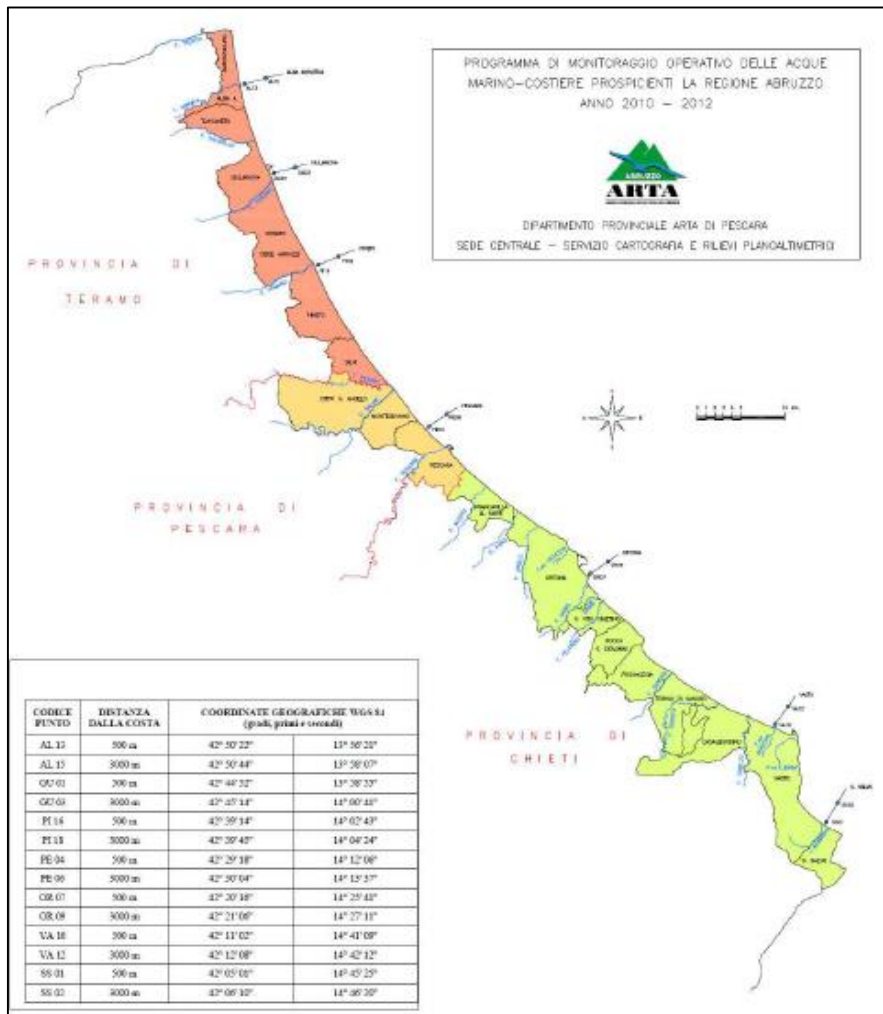


Figure 6: Positioning of monitoring stations in the Abruzzo Network (ARTA).

The monitoring network of ARPAV in the lagoons of the Po delta acquires data in real time, and it is composed by 9 more parametric probes. The data relating to the last 48 hours are made available live for: Dissolved Oxygen, Water Temperature, Salinity, Chlorophyll a and Ph.

For an interpretation of the data, we refer to the values of the parameters chosen by ARPA. They take into consideration the survival limits and the optimal growth intervals for the fish fauna published in the dissemination manual of the TAPES PHILIPPINARUM Aquaculture series "(publication published by Veneto Agricoltura) since the study area own a mussel farm.

For each station, comparisons were made regarding the monthly and annual data. An example of data from one monitoring station (Rosolina, 18<sup>th</sup> October 2021) are reported below. In the discussion has been reported considerations concerning all the monitoring stations regarding three different analyses: 1\_water monitoring in the lagoons; 2\_water monitoring in the two Mytilidae farms; and 3\_water monitoring in the marine area in front of the beaches.

Table 8: Salinity, pH and Temperature values from the collected data.

Sample	Salinity - ppm				pH				T (°C)			
	Vital Limits		Optimal range		Vital Limits		Optimal range		Vital Limits		Optimal range	
	13	50	25	35	>7,5		7,8	8,2	0	31	16	23
<b>2021_10_18_Ros_0.1</b>	<b>32,93</b>				<b>8,26</b>				<b>16,99</b>			
<b>2021_10_18_Ros_4</b>	<b>33,56</b>				<b>8,26</b>				<b>17,26</b>			
2021_10_19_BBMCa_0.1	29,15				8,25				15,88			
2021_10_19_BBMCa_4	29,11				8,25				15,82			
2021_10_19_BBMCb_0.1	28,92				8,24				16,46			
2021_10_19_BBMCb_4	30,99				8,24				16,64			
2021_10_20_Goro_0.1	25,61				8,38				16,53			
2021_10_20_Goro_4	32,99				8,29				18,05			
P1	28,77				8,33				21,56			
P2	28,77				8,33				21,56			
P3	28,42				8,31				22,17			
P4	28,75				8,34				21,48			
P5	28,74				8,34				21,57			
Montesil A	32,61				8,29				9,12			
Montesil B	32,5				8,28				9,05			
Montesil C	32,65				8,26				9,17			
Montesil D	32,63				8,28				8,84			

#### Stazione Marinetta Ottobre 2021 - Temperatura

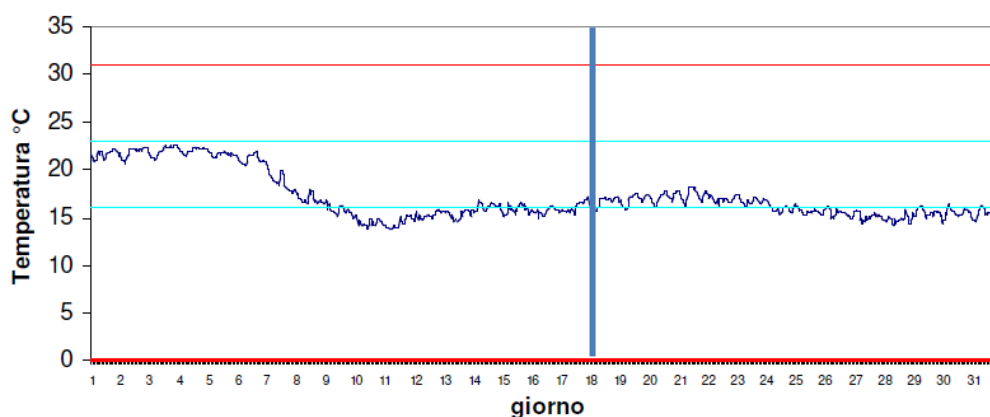


Figure 7: Temperature values of October 2021 (in evidence in blue line the 18th October value) from ARPA data of Stazione Marinetta (Rosolina).

**LAGUNA MARINETTA - TEMPERATURA**

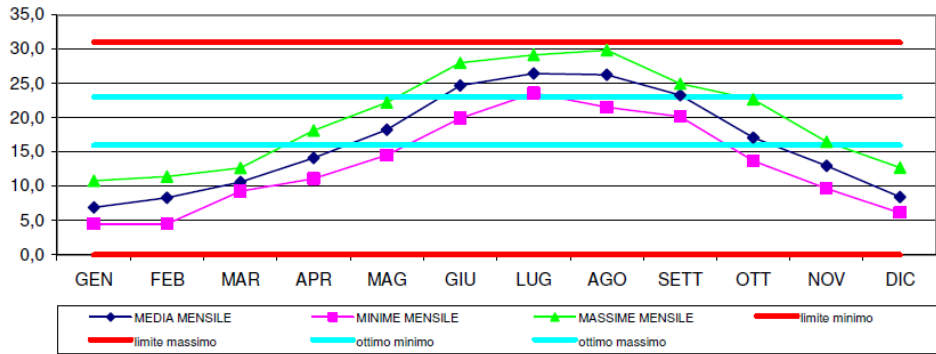


Figure 8: Temperature values-average of the year 2021 from ARPA data of Stazione Marinetta (Rosolina).

**Marinetta -confronto Temperatura  
MEDIA 2015 - 2016 - 2017 - 2018 - 2019- 2020 - 2021**

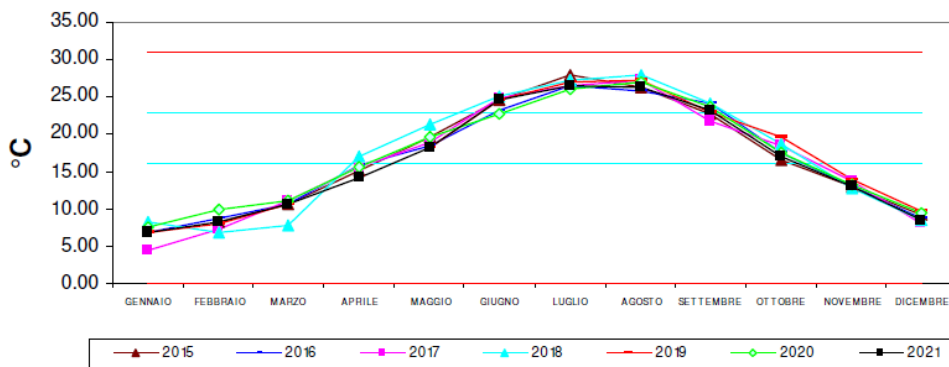


Figure 9: Temperature values-average of the years 2015-2021 from ARPA data of Stazione Marinetta (Rosolina).

**Stazione Marinetta Ottobre 2021 - pH**

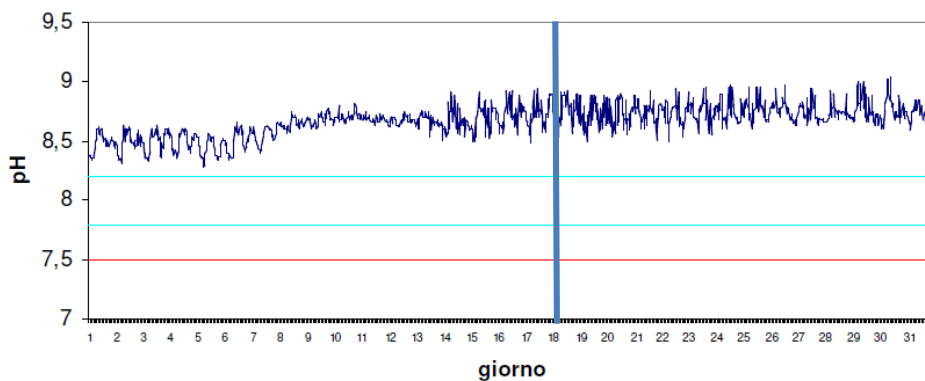


Figure 10: pH values of October 2021 (in evidence in blue line the 18th October value) from ARPA data of Stazione Marinetta (Rosolina).

LAGUNA MARINETTA - pH

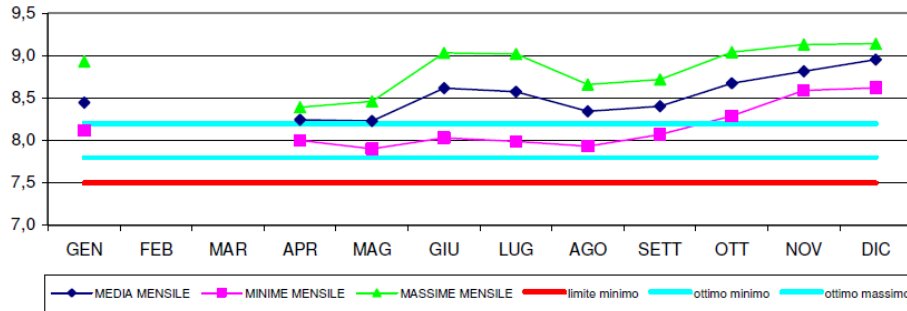


Figure 11: pH values-average of the year 2021 from ARPA data of Stazione Marinetta (Rosolina).

Marinetta - confronto pH  
MEDIA 2015 - 2016 - 2017 - 2018 - 2019 - 2020 - 2021

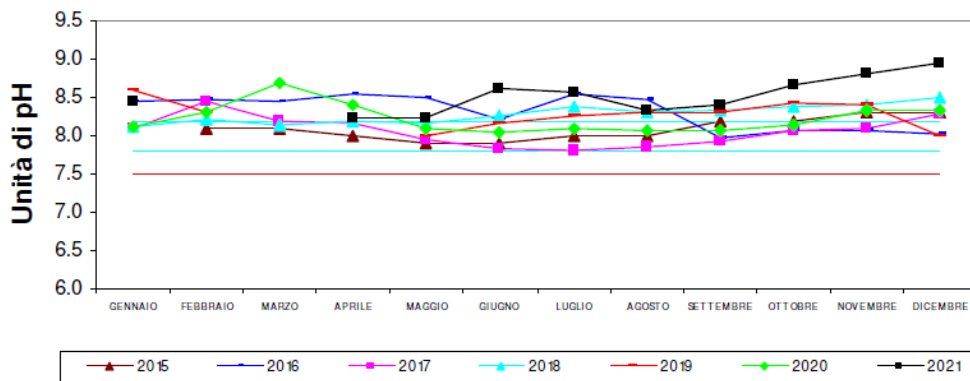


Figure 12: pH values-average of the years 2015-2021 from ARPA data of Stazione Marinetta (Rosolina).

Stazione Marinetta Ottobre 2021 - Conducibilità mS/cm

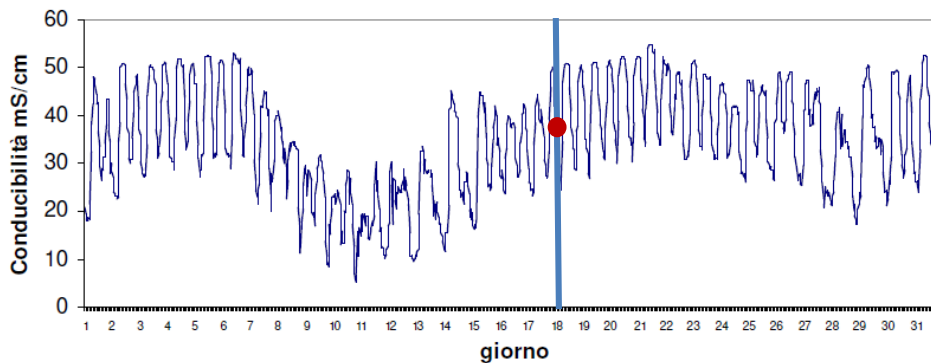


Figura 13: Conductivity values of October 2021 (in evidence in blue line the 18th October value) from ARPA data of Stazione Marinetta (Rosolina).

LAGUNA MARINETTA - CONDUCIBILITA'

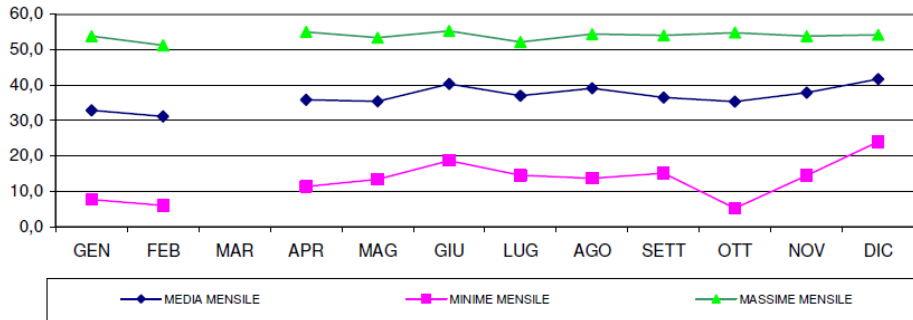


Figure 14: Conductivity values-average of the year 2021 from ARPA data of Stazione Marinetta (Rosolina).

Marinetta - confronto Conducibilità  
 MEDIA 2015 - 2016 - 2017 - 2018 - 2019- 2020 - 2021

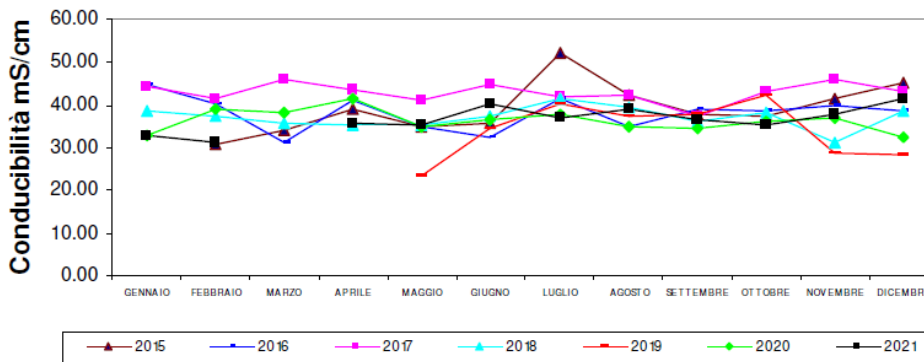


Figure 15: Conductivity values-average of the years 2015-2021 from ARPA data of Stazione Marinetta (Rosolina).

Stazione Marinetta Ottobre 2021 - Salinità %.

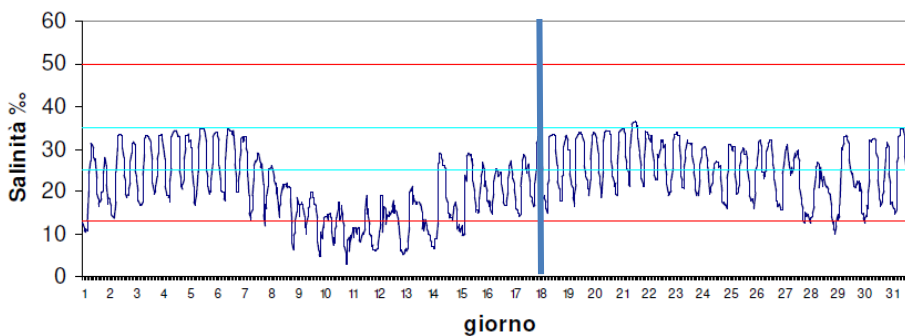


Figure 16: Salinity values of October 2021 (in evidence in blue line the 18th October value) from ARPA data of Stazione Marinetta (Rosolina).

LAGUNA MARINETTA - SALINITA'

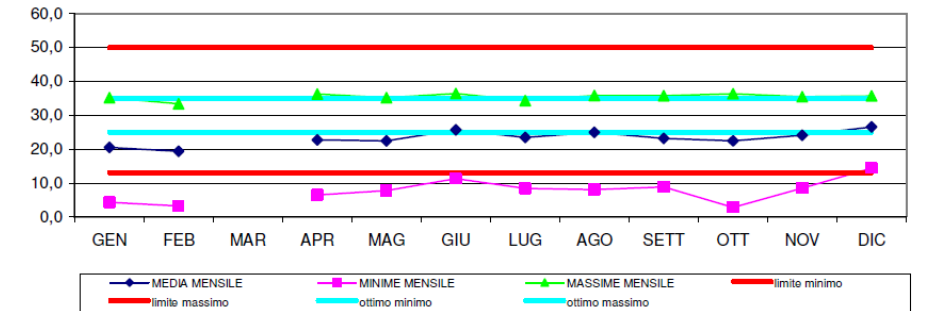


Figure 17: Salinity values-average of the year 2021 from ARPA data of Stazione Marinetta (Rosolina).

Marinetta - confronto Salinità  
MEDIA 2015 - 2016 - 2017 - 2018 - 2019- 2020 - 2021

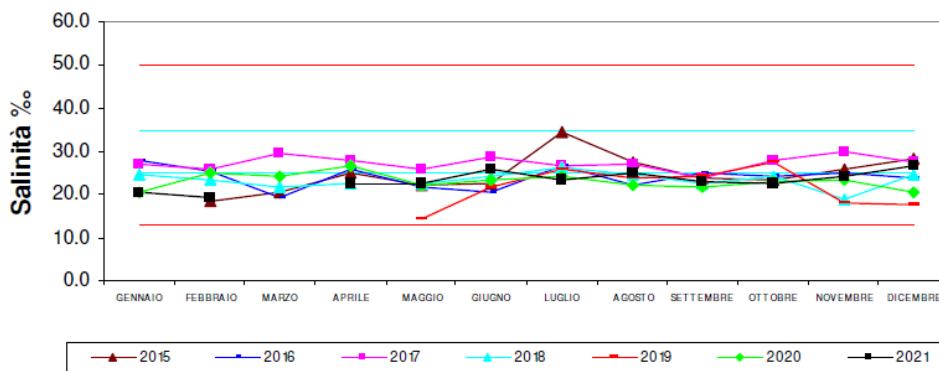


Figure 18: Salinity values-average of the years 2015-2021 from ARPA data of Stazione Marinetta (Rosolina).

Stazione Marinetta Ottobre 2021 - Ossigeno disciolto mg/l

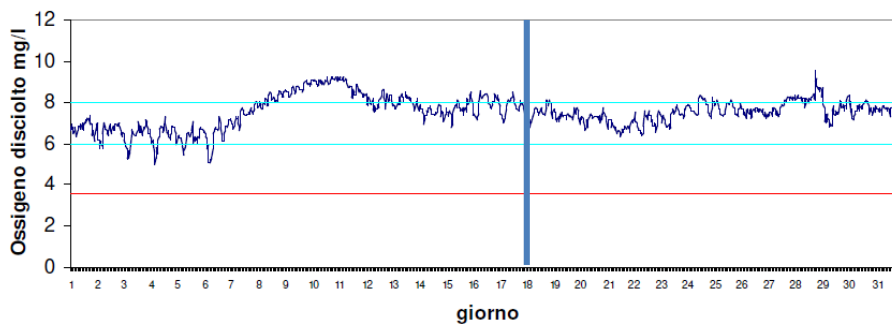


Figure 19: Dissolved Oxygen values of October 2021 (in evidence in blue line the 18th October value) from ARPA data of Stazione Marinetta (Rosolina).

LAGUNA MARINETTA - OSSIGENO DISCIOLTO

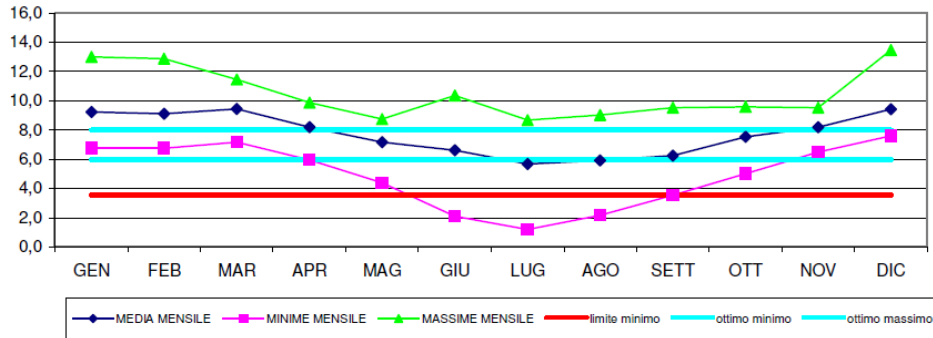


Figure 20: Dissolved Oxygen values-average of the year 2021 from ARPA data of Stazione Marinetta (Rosolina).

Marinetta-confronto Ossigeno disciolto mg/L  
MEDIA 2015 - 2016 - 2017 - 2018 - 2019 - 2020 - 2021

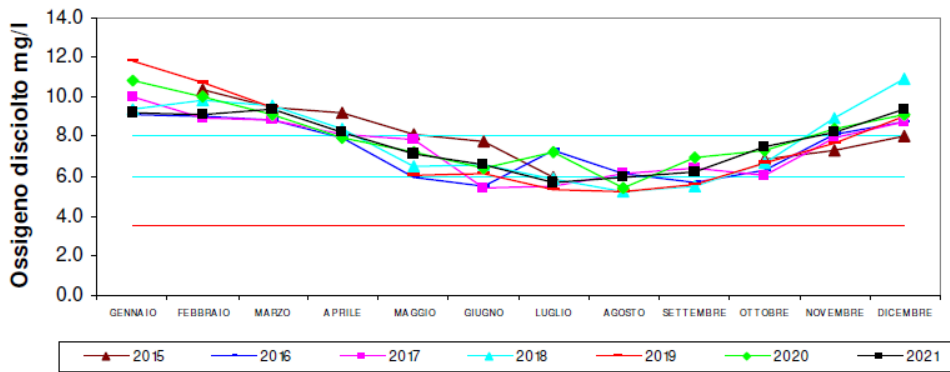


Figure 21: Dissolved Oxygen values-average of the years 2015-2021 from ARPA data of Stazione Marinetta (Rosolina).

2.2.1.2 Ros\_0.1 test site – Discussion of the data

The activities were conducted in a period in which the temperature in the delta lagoons dropped, reducing biological activity. Given the fundamental role of biological organisms in the capture of plastics that tends to colonize the plastic items (*plastisphere*), producing an increase in the size and mass of the particles (Rizzo 2022, PhD thesis), there is a reduction in the accumulation processes in the sediment and consequently a tendency of transferring light microplastics in suspension from the water column to the marine environment. Regarding the salinity, the ARPA data shows that there are high daily fluctuations linked to the tide, which induces ingression and regression of the saline wedge.

The sampling campaign carried out in October 2021 data shows that fresh water inputs, due to heavy rainfall, causes a lowering of salinity below the tolerance limit for the melacofauna present in the lagoon. Future studies would interest the sampling the biota corresponding to the minimum values of salinity, in order to check any variations in the content of microplastics in molluscs.

Fortunately, these events are very short in time, so there is a tolerance and no mollusc deaths are observed. These variations are naturally reflected on the pH, which, in any case, remains high; therefore, no dissolution processes of the carbonates are observed.

The periods with optimal temperature conditions for the biota in the lagoon on Rosolina Mare area are from mid-March to mid-May and from mid-September to mid-October, so in this period there is the maximum chance of transferring the biota that live in lagoon. From mid-May to mid-September the dissolved oxygen in the water is greatly reduced, resulting in eutrophication conditions that favour both the development of algae and microalgae, and the capture and deposition of plastics in the sediments of the lagoon.

The performed observations are similar in all areas of the lagoon in the Po delta.

### 2.2.1.3 Abruzzo region sites – Discussion of the data

The temperatures show high ranges of seasonal variations of similar magnitude across the coast. A high stability of fluctuations is in fact observed on the entire coast, with very cold waters from October to March, but very high temperatures in summer periods. Therefore, there is a considerable thermal stress, which reduces the possibility of development of thermo-sensitive species.

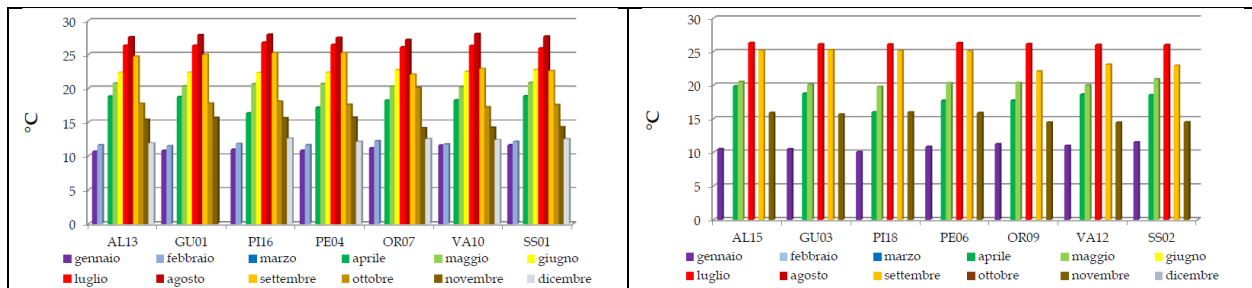


Figure 22: Temperature measured 500 m from the shore (on the left), and 3000 m from the shore (on the right).

There is a low influence of the distance from the coast in the temperature trend. The salinity shows significant variations in the stations of Pescara, both due to the contributions of the rivers and perhaps also to sources fed by the phreatic aquifer emerging on the seabed.



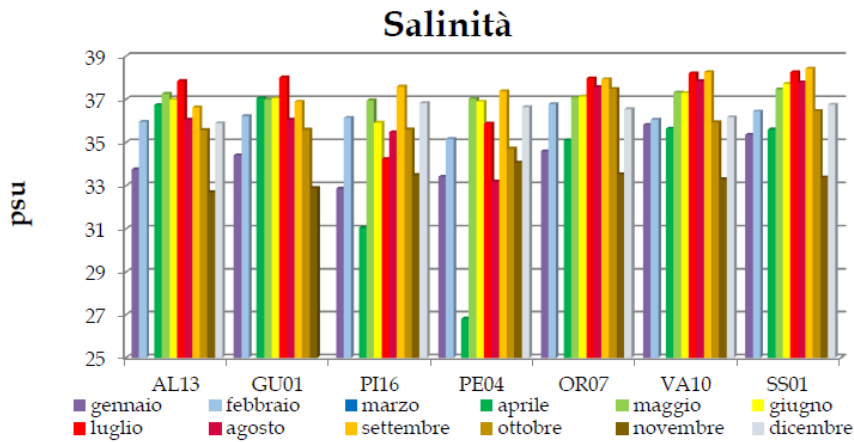


Figura 23: Salinity values of Abruzzo Region.

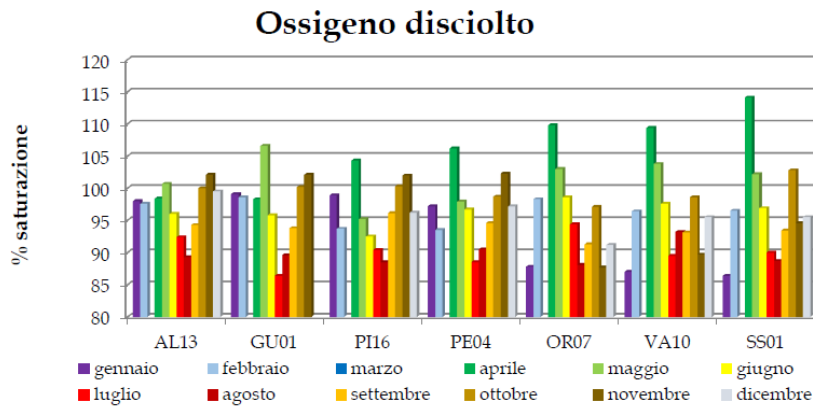


Figure 24: Dissolved oxygen data indicating good availability conditions.

The chemical data detected during the campaigns and compared with the daily surveys performed by ARPA relating to sea water are good, even if they indicate strong seasonal fluctuations with stress during the summer period.

## 2.2.2 Test site 3: Rijeka area (HR)

Physical properties measurements of surface sea water were performed at the same time and at the same locations where the samples of microplastics from the sea surface and samples of mussels were collected except for the transparency measurement which were performed only during collection of microplastics from surface sea water. Different probes were used to measure pH, salinity and oxygen concentration in the sea water. The measurements were obtained in situ or in the laboratory after sampling. Transparency of sea water was measured in situ by using Secchi disk. Locations are described in details in the Deliverable 4.1.1 (*Table 9, Table 10*).

*Table 9: Dates and sampling locations of physical measurements obtained during sampling of microplastics in sea water surface.*

Sampling location	Geographical coordinates	Dates of sampling
<i>Soline bay</i>	45.164073836 N 14.61571733 E	10/06/2021 27/10/2021
<i>Lopar</i>	44.818142 N 14.548351 E	26/05/2021 24/09/2021
<i>Susak</i>	44.818142 N 14.743231 E	28/07/2021 28/09/2021
<i>Vinodolski kanal – Crikvenica - Novi Vinodolski</i>	45.126460 N 14.733594 E	10/06/2021
<i>Vinodolski kanal - Šilo</i>	45.161218 N 14.662726 E	10/06/2021
<i>Krčki most</i>	45.2484727 N 14.5697527 E	10/06/2021 27/10/2021
<i>Omišalj</i>	45.208086 N 14.549098 E	04/05/2022

*Table 10: Dates and sampling locations of physical measurements obtained during sampling of mussels.*

Sampling location	Geographical coordinates	Date of sampling
<i>Lopar</i>	44.823901 N 14.752949 E	24/09/2021 02/02/2022
<i>Bakar</i>	45.306629 N 14.535454 E	08/02/2022 04/05/2022
<i>Smokvica</i>	45.086883 N 14.847759 E	03/05/2022
<i>Stinica</i>	44.726567 N 14.896468 E	03/02/2022

Methods used for physical measurements are standardised ISO methods, as described at the beginning of this chapter.

Temperature of surface sea water ranged from 10°C in February in 2022 in Stinica to 25.6°C measured in Susak in July 2021. The temperature had its usual values for this part of Adriatic Sea and for the season. Transparency ranged from 11m to 17m. Values recorded for pH ranged from 7.8 to 10.15. Values for the dissolved oxygen ranged from 8.01mg/L to 10.15mg/L. Salinity had its usual values and ranged from 25.7 to 38.3‰ (Table 11 and Table 12).

Table 11: Physico-chemical indicators of sea water surface (0.5m depth) measured during microplastics sampling.

Location	Date	Temperature (°C)	Transparency (Secchi disk - m)	pH	Dissolved oxygen (mg/L)	Salinity (‰)
Uvala Soline	10/06/2021	22.4	10 (bottom)	8,0	9,05	34,4
	27/10/2021	17.1	8 (bottom)	7,9	9,25	34,3
Lopar	26/05/2021	17.8	17	7,9	10,01	35,3
	24/09/2021	21.5	12	7,8	9,94	35,9
Susak	28/07/2021	25.6	15	8,0	10,05	37,0
	28/09/2021	22.9	13	8,1	10,15	34,8
Crikvenica	10/06/2021	20.1	13	8,0	9,82	33,4
Šilo	10/06/2021	20.5	11	7,9	9,97	34,3
Omišalj	04/05/2022	15.7	-	8,0	8,01	38,3

Table 12: Physico-chemical indicators of sea water surface (0.5m depth) measured on locations where mussels were sampled.

Location	Date	Depth (m)	Temperature of sea water (°C)	Salinity (‰)	pH	Dissolved oxygen (mg/L)
Lopar	24/09/21	0,5-1	18	35.3	7.9	9.75
Stinica	03/02/22	0,5	10	34.2	7.8	9.89
Bakar	08/02/22	0,3	11	25.7	7.9	9.89
Lopar	02/02/22	0,5	11	33.2	8,0	9.76
Smokvica	03/05/22	0,5	12	34.7	7.9	10.03
Bakar	04/05/22	0,5	11	26.8	7.8	9.82

When we compare values obtained from this study with the other studies (*Errore. L'origine riferimento non è stata trovata.* and *Errore. L'origine riferimento non è stata trovata.*) it is noticeable that the values are not very different and have similar ranges. There is a slight difference in the values obtained for the concentration of oxygen in the sea water, but that could be partly the consequence of using different probes in the two studies which are calibrated differently. From "Prostorni plan" of Primorje Gorski kotar County it is visible that the sea surface temperature in the Gulf of Rijeka is at its minimum in February/March, and reaches its maximum in August. The influence of the inflow of fresh water in the area of the Kvarner Gulf is significant and is most pronounced in the northern part of the Rijeka Gulf, where the surface salinity varies between 23.00‰ and 37.00‰. In other parts of the Gulf of Rijeka, including Srednja and Vela vrata, salinity variations are less pronounced and range from 32.6-38.1‰. The salinity in the area of Kvarner and Kvarnerić is mostly around 36.5‰, but in periods of the strongest inflow of fresh water, a lower salinity of 35.00‰ is also possible. Transparency values are highly variable and range from 0.5-31 m. Transparency in the area of Cres and Lošinj varies between 7 and 32

m. The oxygen concentration varies and oxygen saturation on the surface during significant photosynthetic activity of flora elements can reach 270% saturation.

Table 13: Physico-chemical properties of Bakarski zaljev obtained from Hrvatske vode (Hrvatske vode, <https://www.voda.hr/en>, 2018.).

Location	GPS coordinates	Date	Depth	Temperature	O <sub>2</sub>	O <sub>2</sub> (%)	pH	Chl $\alpha$
Bakarski zaljev	45,303614 N 14,541153 E	17/04/18	0	12,68	7,31	1,09	8,13	1,82
Bakarski zaljev	45,303614 N 14,541153 E	17/04/18	5	12,03	6,53	1,09	8,27	0,74
Bakarski zaljev	45,303614 N 14,541153 E	17/04/18	10	11,83	6,47	1,08	8,26	0,91
Bakarski zaljev	45,303614 N 14,541153 E	17/04/18	25	11,27	6,31	1,04	8,25	1,38
Bakarski zaljev	45,303614 N 14,541153 E	22/08/18	0	22,50	5,32	1,05		0,31
Bakarski zaljev	45,303614 N 14,541153 E	22/08/18	5	22,80	5,63	1,16		0,33
Bakarski zaljev	45,303614 N 14,541153 E	22/08/18	10	21,42	5,75	1,16		0,28
Bakarski zaljev	45,303614 N 14,541153 E	22/08/18	24	15,55	6,13	1,11		0,27
Bakarski zaljev	45,303614 N 14,541153 E	08/11/18	0	13,29	7,12	1,14		0,26
Bakarski zaljev	45,303614 N 14,541153 E	08/11/18	5	17,16	5,31	0,99		0,27
Bakarski zaljev	45,303614 N 14,541153 E	08/11/18	10	17,15	5,16	0,96		0,32
Bakarski zaljev	45,303614 N 14,541153 E	08/11/18	25	17,12	5,08	0,95		0,22
Bakarski zaljev	45,303614 N 14,541153 E	11/12/18	0	13,32	5,95	0,96		1,10
Bakarski zaljev	45,303614 N 14,541153 E	11/12/18	5	15,18	5,28	0,95		1,06
Bakarski zaljev	45,303614 N 14,541153 E	11/12/18	10	14,97	5,17	0,93		1,11
Bakarski zaljev	45,303614 N 14,541153 E	11/12/18	25	14,31	4,98	0,88		0,12

Table 14: Physico-chemical properties of Luka Rijeka obtained from Hrvatske vode (Hrvatske vode, <https://www.voda.hr/en>, 2018.).

Location	GPS coordinates	Date	Depth	Temperature	O2	O2 (%)	pH	Chl <i>a</i>
Luka Rijeka	45,303614 N 14,541153 E	18/04/18	0	14,41	6,13	1,06	8,21	0,49
Luka Rijeka	45,303614 N 14,541153 E	18/04/18	5	13,60	6,34	1,10	8,23	0,43
Luka Rijeka	45,303614 N 14,541153 E	18/04/18	10	13,00	6,46	1,11	8,24	0,48
Luka Rijeka	45,303614 N 14,541153 E	18/04/18	55	10,31	5,72	0,93	8,21	0,45
Luka Rijeka	45,303614 N 14,541153 E	23/08/18	0	23,85	5,08	1,07		0,19
Luka Rijeka	45,303614 N 14,541153 E	23/08/18	5	22,05	5,49	1,12		0,18
Luka Rijeka	45,303614 N 14,541153 E	23/08/18	10	20,10	5,81	1,15		0,18
Luka Rijeka	45,303614 N 14,541153 E	23/08/18	55	11,00	4,32	0,71		0,23
Luka Rijeka	45,303614 N 14,541153 E	09/11/18	0	14,08	6,16	1,05		0,32
Luka Rijeka	45,303614 N 14,541153 E	09/11/18	5	17,28	5,39	1,01		0,31
Luka Rijeka	45,303614 N 14,541153 E	09/11/18	10	17,29	5,29	0,99		0,34
Luka Rijeka	45,303614 N 14,541153 E	09/11/18	55	14,76	5,05	0,90		0,30
Luka Rijeka	45,303614 N 14,541153 E	12/12/18	0	9,31	5,87	0,88		0,37
Luka Rijeka	45,303614 N 14,541153 E	12/12/18	5	13,86	5,56	0,97		0,37
Luka Rijeka	45,303614 N 14,541153 E	12/12/18	10	14,19	5,39	0,95		0,41
Luka Rijeka	45,303614 N 14,541153 E	12/12/18	55	14,13	4,86	0,86		0,11

### 2.2.3 Test site 4: Split area (HR)

In the Split area PP8 (University of Split - FGAG) focalized the sampling campaigns mainly in relation to the presence of microplastic and their principal sources in this specific area (wastewater). In fact, here the wastewater effluent contains high concentrations of pollutants including microplastics, which can cause a large amount of deterioration to marine environments. Bacteria are the most abundant and diverse group of organisms living in the wastewater and bathing water status is mainly determined using fecal indicator bacteria, as indicators of water quality and related human health issues. Besides fecal pollution, microplastic of different sizes is another important aspect of coastal water quality, leading jointly to the eutrophication problems in coastal waters. Since primary producers are the first components of the ecosystem to react to an increase in nutrient concentration, phytoplankton biomass is considered a good indicator of the trophic state of the coastal water. Changes in the phytoplankton biomass abundance occur following nutrient enrichment, which can happen naturally (through riverine influence or upwelling of nutrients from the bottom) or under anthropogenic influence (urban and industrial wastewater discharges and surface runoff). Anthropogenically introduced nutrients and other pollutants are the major problem of coastal ecosystems and their mixing with seawater contributes to the eutrophication of the coastal zone waters.

For these reasons, in the Split area the measurements were performed with the CTD fast profiling probe, and C3 fluorometer, during sampling sessions conducted with the boat (Nautica 600) every month from February to September 2020 (with exception of March and August due to the COVID restrictions).

The Sea & Sun Technology CTD fast profiling probe with an additional sensor for dissolved oxygen (model: 48M) was used for temperature, salinity, density anomaly, and dissolved oxygen measurements. Density anomaly was calculated automatically by CTD/DO probe internal software using the international thermodynamic equation of seawater-2010 [52]. Turbidity, chlorophyll, and colored dissolved organic matter (CDOM) were measured using a C3 Submersible fluorometer (Turner Design). Chlorophyll measurements are performed with a blue mercury lamp, with peak emission at 460 nm, and fluorescence collected at 680 nm. CDOM was measured using a UV LED, with peak emission at 350 nm and fluorescence collection at 450 nm. Turbidity was measured with the IR lamp, with peak emission at 850 nm, and the collection of scattered light at 90°. Since the relationship between phytoplankton biomass and chlorophyll fluorescence is highly variable and depends on the physiological state and community composition, in this study, we focused on the general distribution of chlorophyll profiles in the water column concerning the stratification and effluent discharge.

The main results from six sampling cruises are presented in the following **Errore. L'origine riferimento non è stata trovata.** and **Errore. L'origine riferimento non è stata trovata.** for location 1 and location 2, respectively. Each Figure contains six vertical profiles corresponding to the sampling month with the set of parameters measured. Analysis of the buoyancy frequency showed that stratification occurred in May, June, July, and September for both locations. In February and April, the winter and early spring, lower temperatures induced vertical mixing in the water column. As a result of the strong sea surface warming, the shallowest stratification occurred in July, while the deepest occurred in September.

At both locations 1 and 2, temperature and salinity followed their seasonal pattern, with low gradients in winter and steeper during stratified periods.

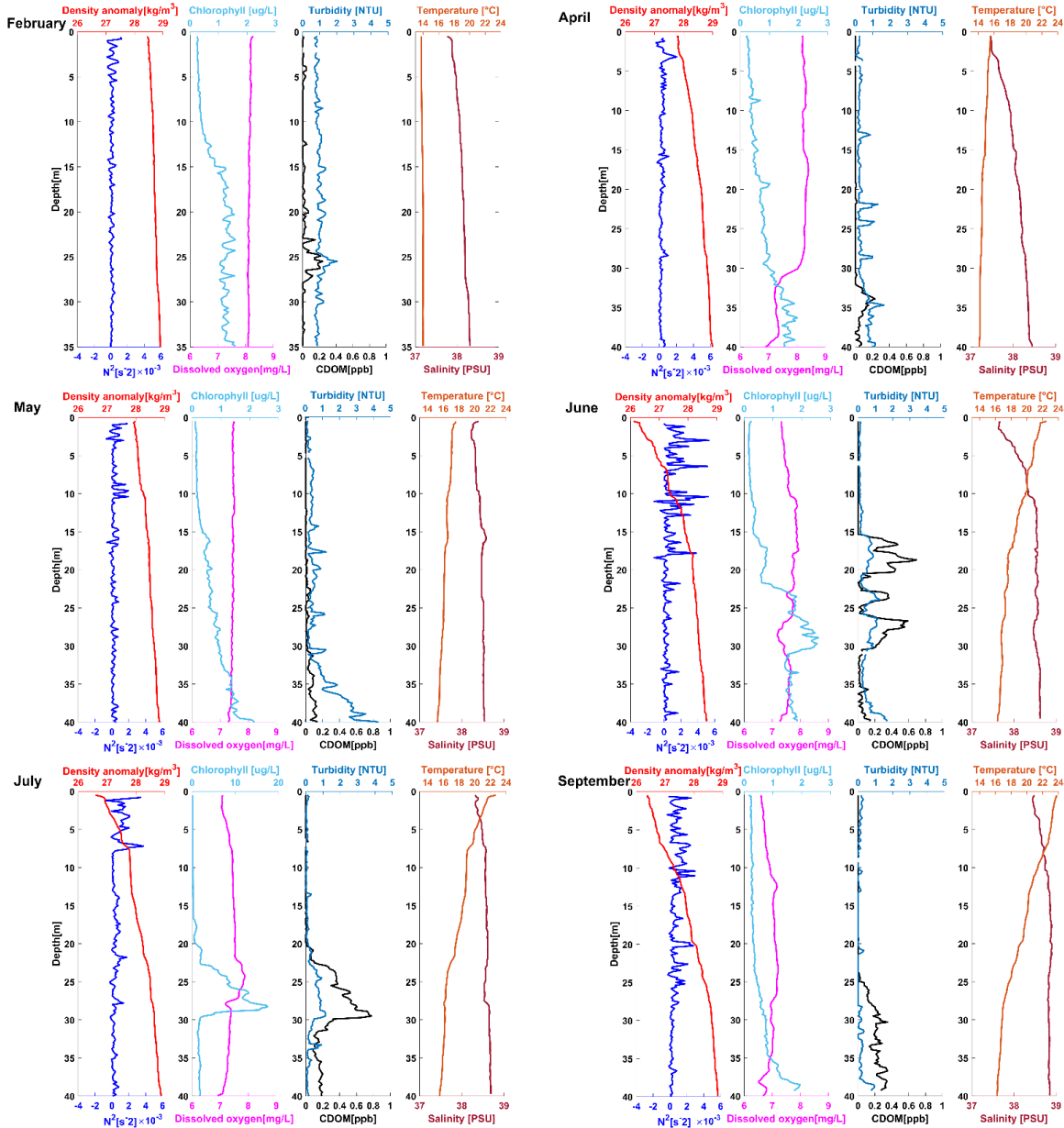


Figure 25: Vertical profiles were sampled during 2020 at location 1. The measured parameters are density anomaly (red line), buoyancy frequency (blue line), chlorophyll (light blue line), dissolved oxygen (magenta line), turbidity (green line), CDOM (black line), temperature (orange line), and salinity (brown line).

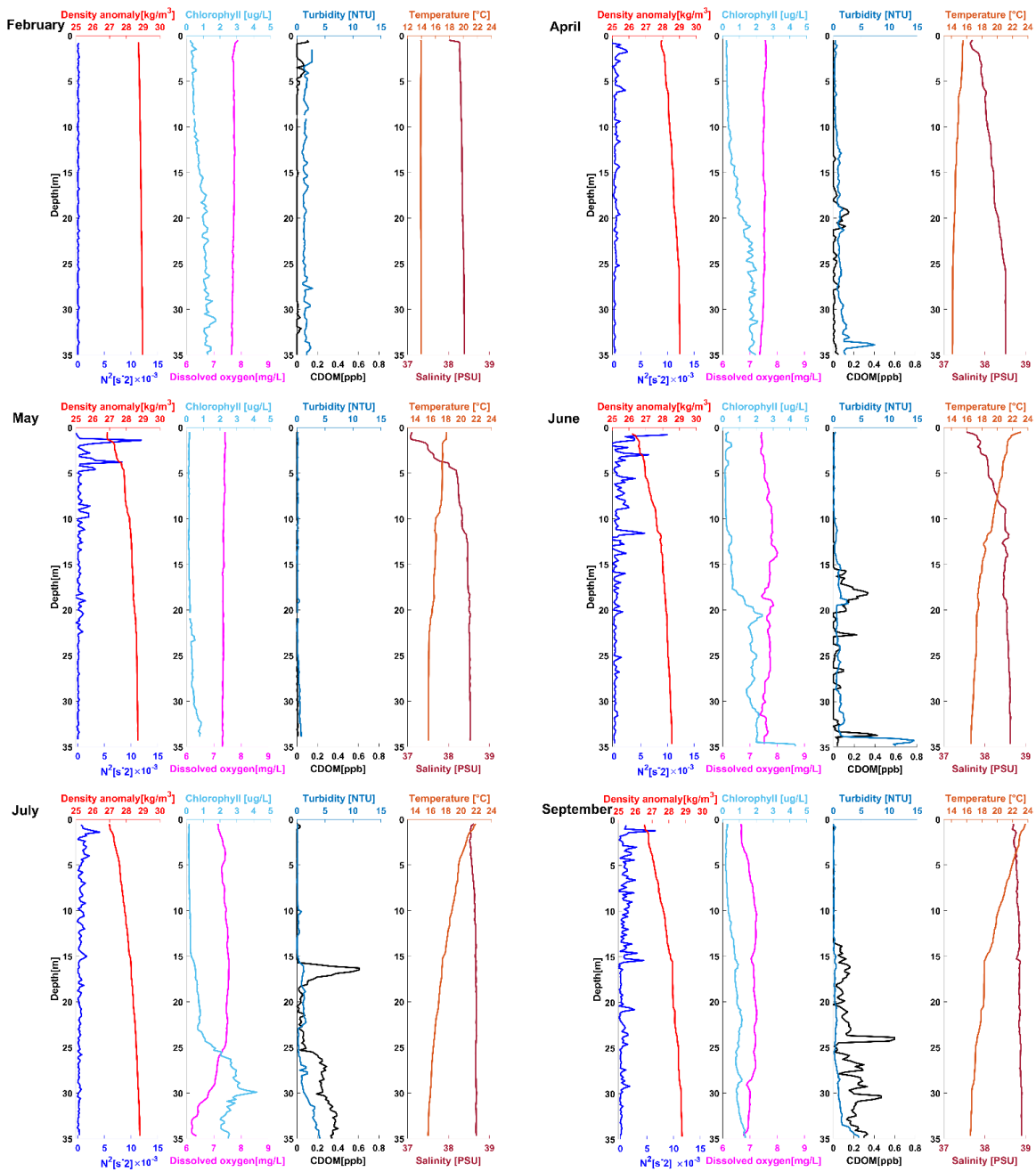


Figure 26: Vertical profiles were sampled during 2020 at location 2. The measured parameters are density anomaly (red line), buoyancy frequency (blue line), chlorophyll (light blue line), dissolved oxygen (magenta line), turbidity (green line), CDOM (black line), temperature (orange line), and salinity (brown line).



The University of Split also studied the wastewater impact on the chlorophyll vertical distribution. Measurements were performed in the eastern central Adriatic Sea, on two locations of marine outfalls, near the city of Split in Croatia. They described the three vertical chlorophyll profile types, based on the stratification conditions and the effluent plume presence. The water column mixing induced the upwelling of the bottom water and enabled the rise of the effluent towards the surface. In the stratified conditions categorized as the ECP type, the pycnocline prevents the plume from rising, keeping it in the lower part of the water column, while the BCP type of profile represents a case when the water column is stratified, but no effluent plume is present. Their categorization of the different vertical chlorophyll profiles is supported by data collected by the Croatian water agency at the locations unaffected by the marine outfalls. All three observed chlorophyll profile types are the consequence of the interplay between the physical, biological, and chemical processes. To distinguish these processes and confidently identify the presence of the effluent plume we use the FIB measurements, along with dissolved oxygen gradients to examine the conditions when oxygen consumption exceeds the production, indicating organic matter oxidation. This, together with salinity, CDOM, and turbidity measurements allows us to separate the wastewater influence from the natural processes. We confirm the importance of the stratification in submerging the effluent below the pycnocline, which is highlighted in February 2020 when column mixing allowed the FIB to rise to the surface of the water column. To our knowledge, this is the first study involving in situ vertical measurements coupled with the submarine outfall analyzing its influence on the vertical chlorophyll distribution.

The water column mixing induced the upwelling of the bottom water generating, and enabled the rise of the effluent towards the surface. In the stratified conditions, the pycnocline prevents the plume from rising, keeping it in the lower part of the water column. During the period from October until May, the Easter Central Adriatic Sea is predominantly unstratified enabling the effluent plume to reach the surface carrying a major source of microplastics to spread laterally due to the wind and sea current conditions. The importance of the stratification in submerging the effluent below the pycnocline is often the natural way of preserving the surface sea layers from the introduction of microplastics from wastewater effluent.

PP7 (RERA) with the support of the Institute of Oceanography and Fisheries (IOR) performed a sampling campaign on July 2<sup>nd</sup> and 3<sup>rd</sup>, 2020, at three transects within the Easter Central Adriatic Sea. The locations of selected transects are shown in Figure below.

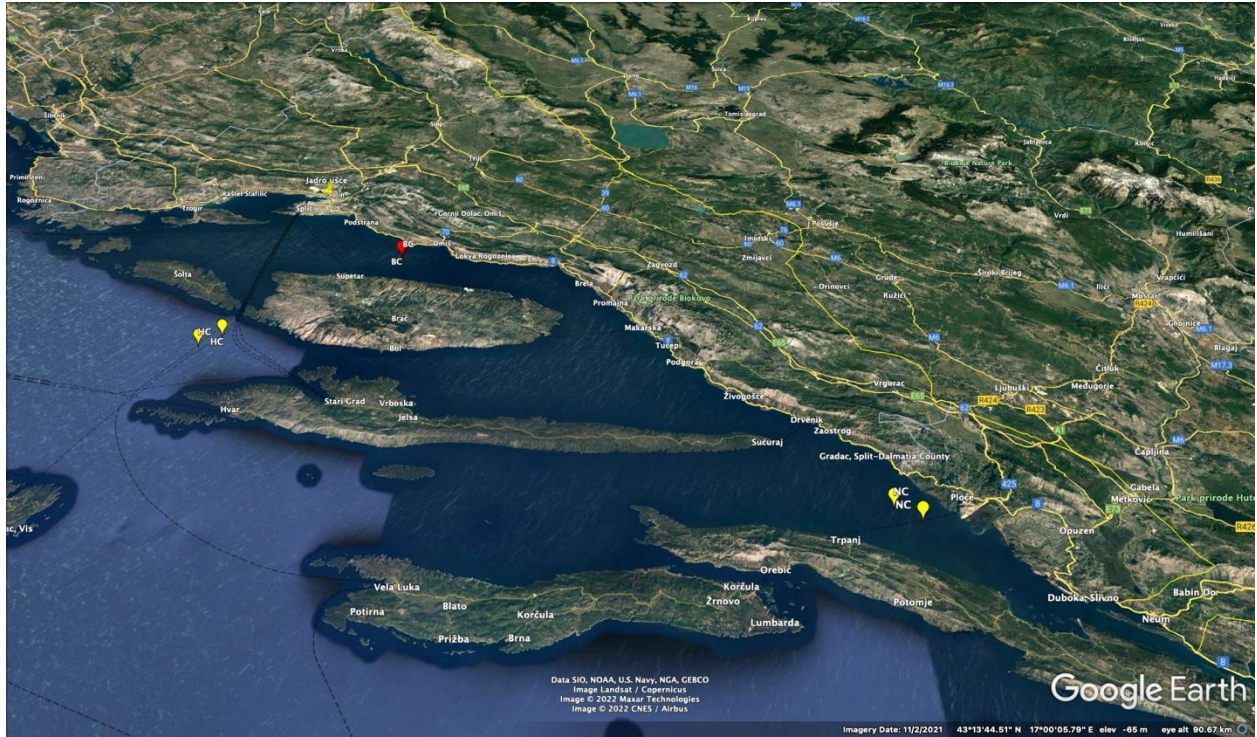


Figure 27: Location of three transects sampled for microplastics and Physico-chemical parameters (Split area)



Figure 28: Two transects (BC and HC) within the city of Split coastal waters (a) and transect (NC) in the river Neretva estuary.

Two sampling transects within the city of Split coastal waters are shown in *Figure 28 (left)*, while the third transect is in the estuary of river Neretva in *Figure 28 (right)*. The three transects are then identified as follows:

- Transect 1. Brač channel (BC)
- Transect 2. Hvar channel (HC)
- Transect 3. Neretva channel (NC)



*Figure 29: Sampling the Physico-chemical parameters during the campaign in July, 2020.*

The Physico-chemical measurements were performed with the CTD fast profiling probe and C3 fluorometer. The Sea & Sun Technology CTD fast profiling probe with an additional sensor for dissolved oxygen (model: 48M) was used for temperature, salinity, density anomaly, and dissolved oxygen measurements. Density anomaly was calculated automatically by CTD/DO probe internal software using the international thermodynamic equation of seawater-2010. Turbidity, chlorophyll, and colored dissolved organic matter (CDOM) were measured using a C3 Submersible fluorometer (Turner Design). Chlorophyll measurements are performed with a blue mercury lamp, with peak emission at 460 nm, and fluorescence collected at 680 nm. CDOM was measured using a UV LED, with peak emission at 350 nm and fluorescence collection at 450 nm. Turbidity was measured with the IR lamp, with peak emission at 850 nm, and the collection of scattered light at 90°. Since the relationship between phytoplankton biomass and chlorophyll fluorescence is highly variable and depends on the physiological state and community composition, in this study, we focused on the general distribution of chlorophyll profiles in the water column at the beginning and at the end of each transect also used for the microplastics measurements.

The main results for Physico-chemical parameters from the sampling cruise are presented in vertical profiles of 5 m depth at the beginning and the endpoint of each transect. The results are shown below and grouped as beginning and end of the transects in the next 6 figures, for transects corresponding to BC, HC, and NC, respectively. The sampled parameters are Density anomaly [ $\text{kg/m}^3$ ], Chlorophyll [ $\mu\text{g/l}$ ], Dissolved oxygen [ $\text{mg/l}$ ], Turbidity [NTU], Colored dissolved organic matter (CDOM) [ppb], Temperature [ $^{\circ}\text{C}$ ], and Salinity [PSU].

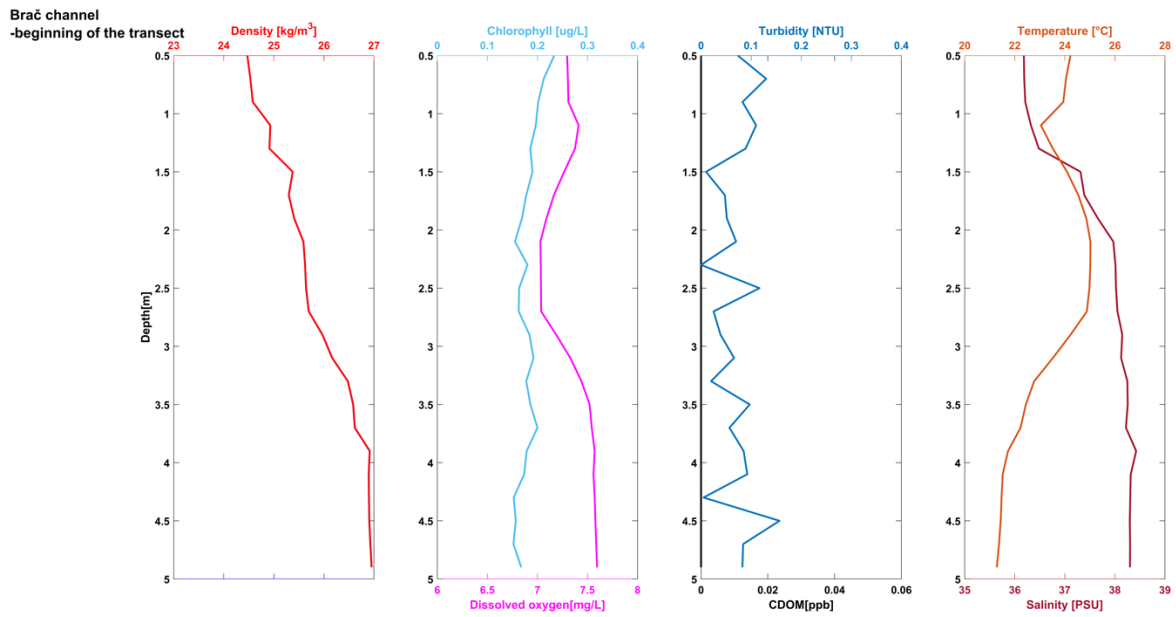


Figure 30: Brač channel - beginning of the transect

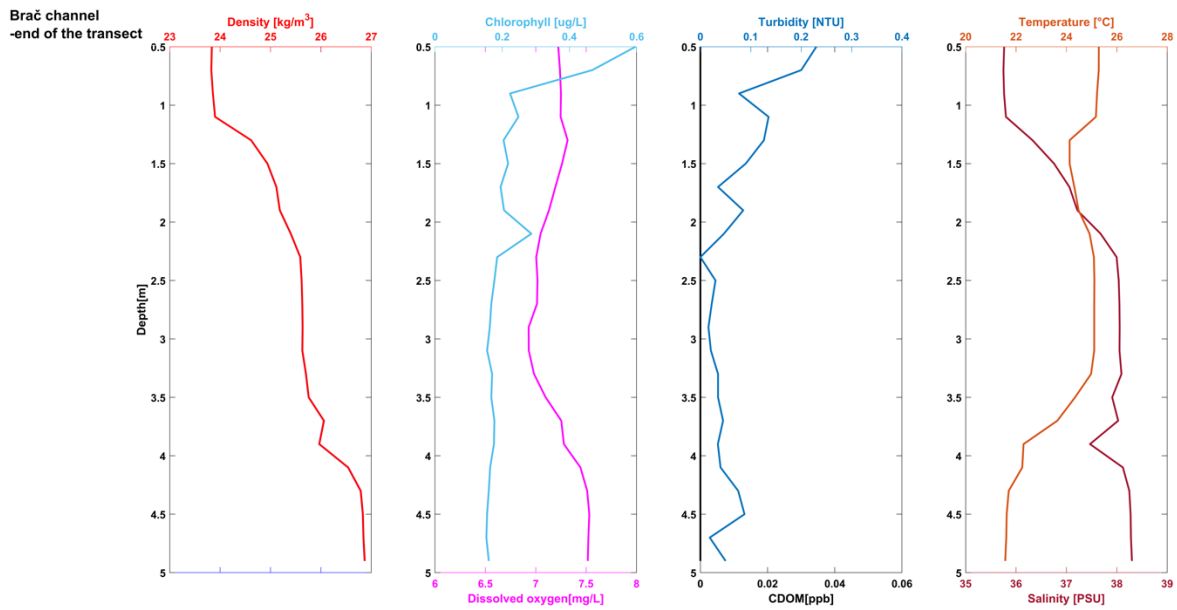


Figure 31: Brač channel - end of the transect

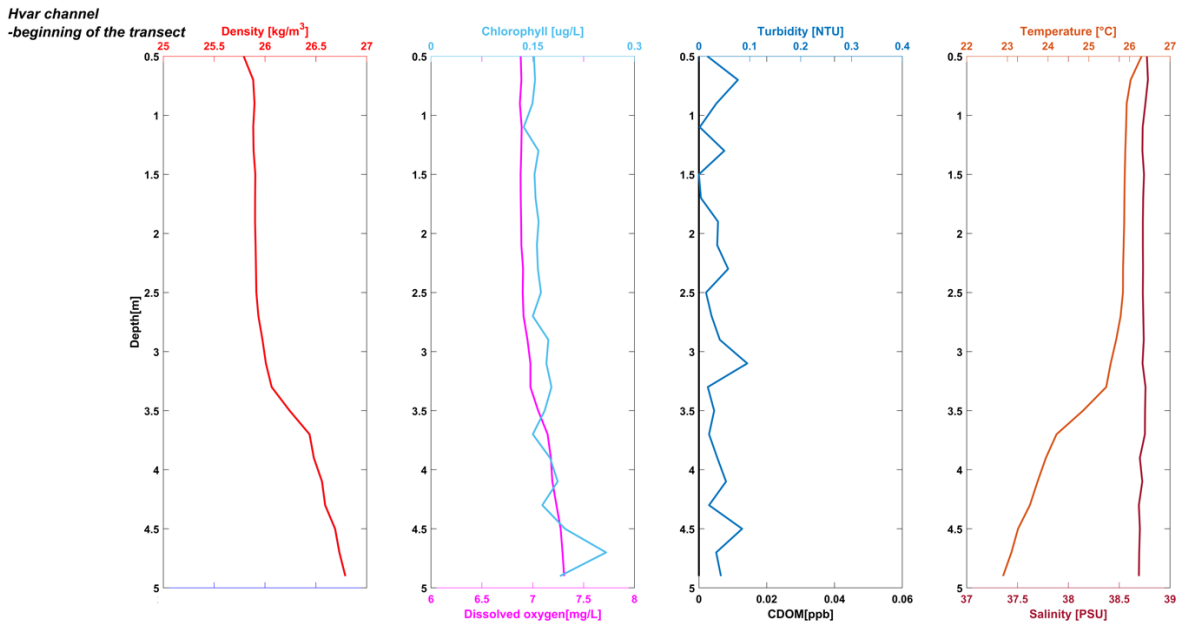


Figure 32: Hvar channel - beginning of the transect

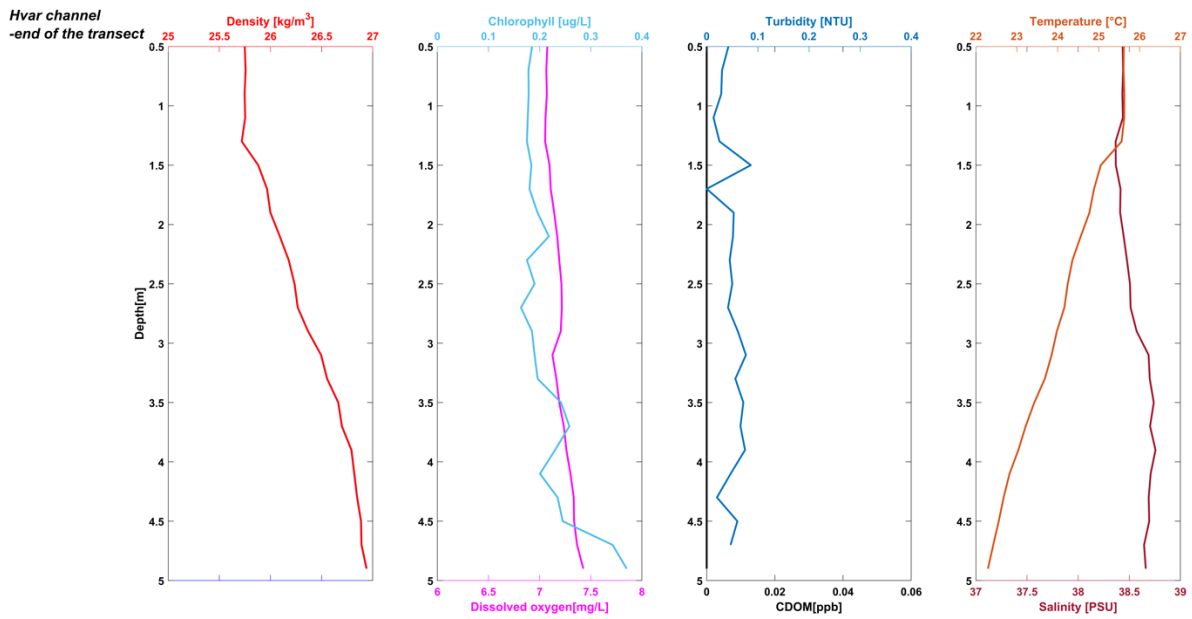


Figure 33: Hvar channel - end of the transect

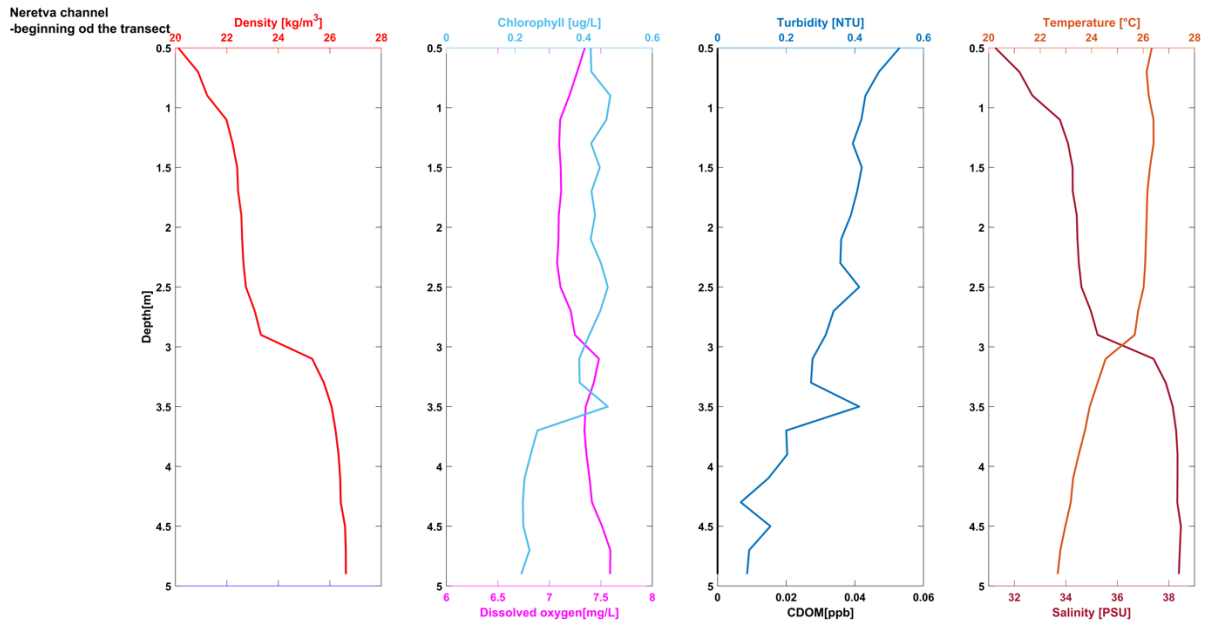


Figure 34: Neretva channel - beginning of the transect

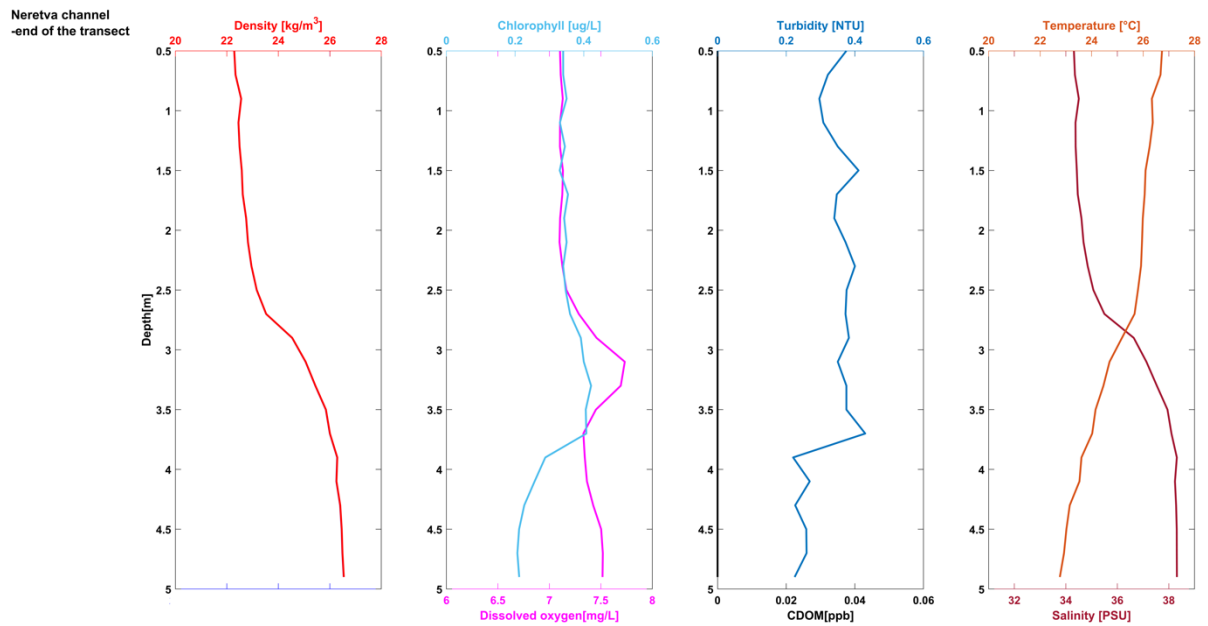


Figure 35: Neretva channel - end of the transect

## 2.3 UAV OBU Marine drone campaign

In three of the Project Pilot sites (Po Delta, Rijeka and Split area) Hydra Solution, with the collaboration of UNIFE, Prosoft, RERA, TIPH performed some sampling campaigns, in order to test the integrated system (*Figure 36*) developed in WP3 and WP5 consisting in an autonomous vehicle (marine drone) equipped with an holo-sensor (SEQUOIA LISST-HOLO2), a mini manta, and an OBU – On Board Unit (probes) (*Figure 38*).

The main information related to the sampling carried out in the areas of Po Delta, Rijeka and Split with the integrated system of the marine drone are described in the following Table.

*Table 15: Main characteristics of the marine drone campaigns.*

Date	Site	Holo-sensor	OBU	Mini-manta	Note
23/10/2021	Volano	X		X	Integrated system testing phase. Manta: 1 transect/15min
27/10/2021	Rijeka	X	X	X	Manta: 2 transect/15 and 30min OBU: on board of the ship
29/10/2021	Split	X	X	X	Manta: 2 transect/30 min OBU: on board of the ship
04/05/2022	Rijeka		X	X	Manta: 2 transect/30 min OBU: mounted on marine drone
12/05/2022	Goro		X	X	Manta: 2 transect/30min OBU: mounted on marine drone

Data collected with Lisst-Holo2 fixed below the drone hull and with the OBU equipped with CTD are reported in the following pages. For each campaign a table summarizes the mission parameters, a table with plot shows the MPs distribution and a table shows the CTD data.

In the missions carried out in October 2021 the system configuration was the following with the OBU equipped with CTD mounted on board of the boat (*Figure 37*).

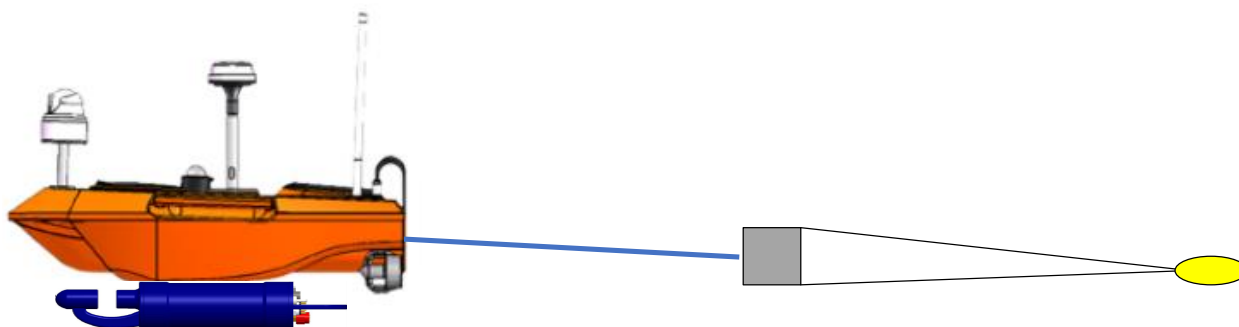


*Figure 36: Integrated system configuration.*



Figure 37: Integrated system on field (Marine drone + holo-sensor + mini manta).



Figure 38: OBU with CTD and GNSS used on board of the boat.

In the missions carried out in May 2022 the drone was equipped only with the manta thus the MPs data are only the one obtained with laboratory analysis whereas the OBU was equipped also with Turbidity and Dissolved Oxygen sensors.



### 2.3.1 Volano field campaign – October 2021 (Po Delta)

The first campaign performed with the marine drone system has been carried out in Volano (Ferrara, IT). In this case the integrated system was deployed from the beach, and the holo-sensor data and mini-manta samples have been acquired along 1 transect starting from the seashore toward SE (recording of 15 minutes).

Table 16: Information related to the holo-sensor recording in Volano.

Mission Name	GORO
Location	FERRARA (IT)
Time Begin	23/10/2021 10:15
Duration	00:15:15
Path Length	0.5km
Average speed	2.0km/h
Holograms collected at 20fps	18312
Holograms with particles	152
Particles Detected	1305
Particles that are clearly plankton or fish eggs	215
Linear concentration [Particles/km]	2180 particles/km
Volume concentration [Vol Particles / Vol Processed]	19.31ul/l

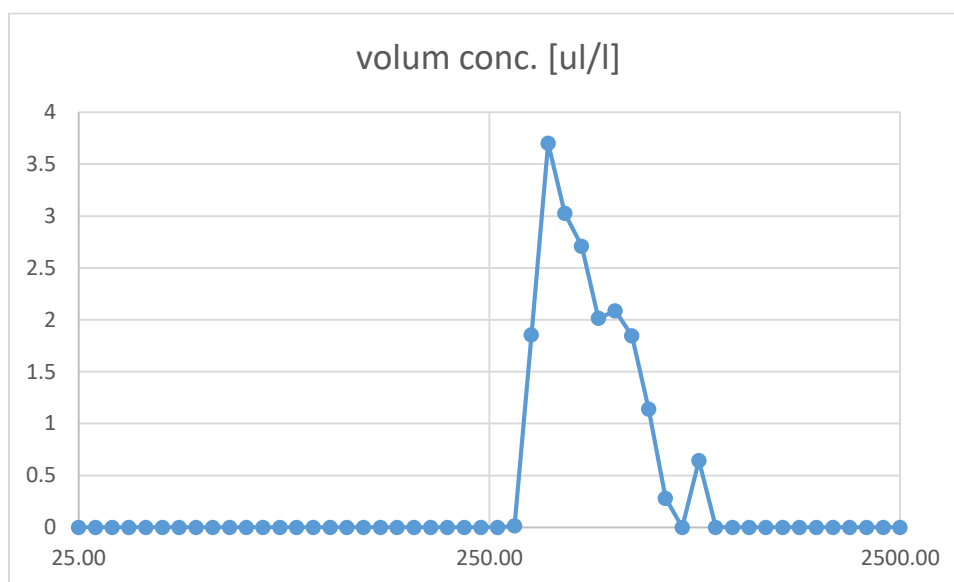


Figure 39: Volano MPs volume distribution

### 2.3.2 Rijeka field campaign – October 2021 (Rijeka area)

The second campaign performed with the marine drone system has been carried out in two different locations in Rijeka (HR). In this case the integrated system was deployed from the boat, and the holo-sensor data and mini-manta samples have been acquired along 2 transect (recording of 15 and 30 minutes). In the first case the duration was reduced due to the presence of a strong upstream current and high waves (>30 cm) that prevented the continue of the transect acquisition. OBU system recorded the physical properties and was installed on the boat.

Table 17: CTD data recorded by OBU system from the boat in Rijeka.

DATE	TIME	LAT	LON	TW[°C]	CW[mS/cm]	SW[ppt]
27/10/21	15:45:44	45.247300	014.577150	15.50	48.00	33.70
27/10/21	15:45:47	45.247300	014.577100	15.50	48.00	33.70
27/10/21	15:45:50	45.247300	014.577050	15.50	48.00	33.70
27/10/21	15:45:53	45.247300	014.577000	15.50	48.00	33.70
27/10/21	15:45:56	45.247300	014.576933	15.50	48.00	33.70
27/10/21	15:45:59	45.247300	014.576900	15.50	48.00	33.70
27/10/21	15:46:03	45.247300	014.576816	15.50	48.00	33.70

Table 18: Information related to the holo-sensor recording in Rijeka (1 transect).

Mission Name	BRIDGE KRK
Location	KRK (HR)
Time Begin	27/10/2021 17:40
Duration	00:17:10
Path Length	1.2km
Average speed	4.2km/h
Holograms collected at 20fps	20392
Holograms with particles	151
Particles Detected	402
Particles that are clearly plankton or fish eggs	148
Linear concentration [Particles/km]	212 particles/km
Volume concentration [Vol Particles / Vol Processed]	8.55ul/l

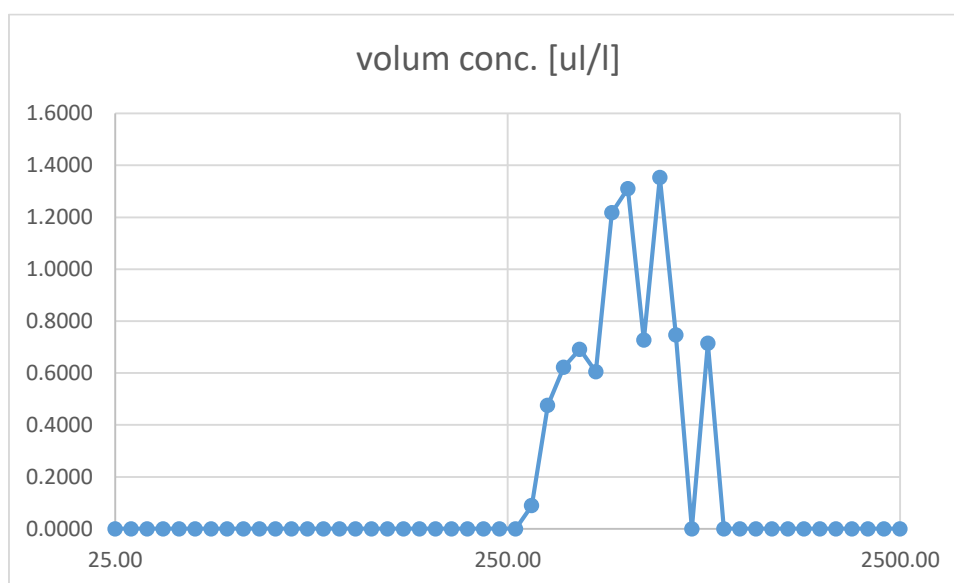


Figure 40: MPs volume distribution in Bridge Krk (Rijeka).

Table 19: Information related to the holo-sensor recording in Rijeka (II transect).

Mission Name	KLIMNO
Location	KRK (HR)
Time Begin	27/10/2021 12:45
Duration	00:33:26
Path Length	1.1km
Average speed	2.0km/h
Holograms collected at 20fps	36949
Holograms with particles	174
Particles Detected	205
Particles that are clearly plankton or fish eggs	92
Linear concentration [Particles/km]	103 particles/km
Volume concentration [Vol Particles / Vol Processed]	3.09ul/l

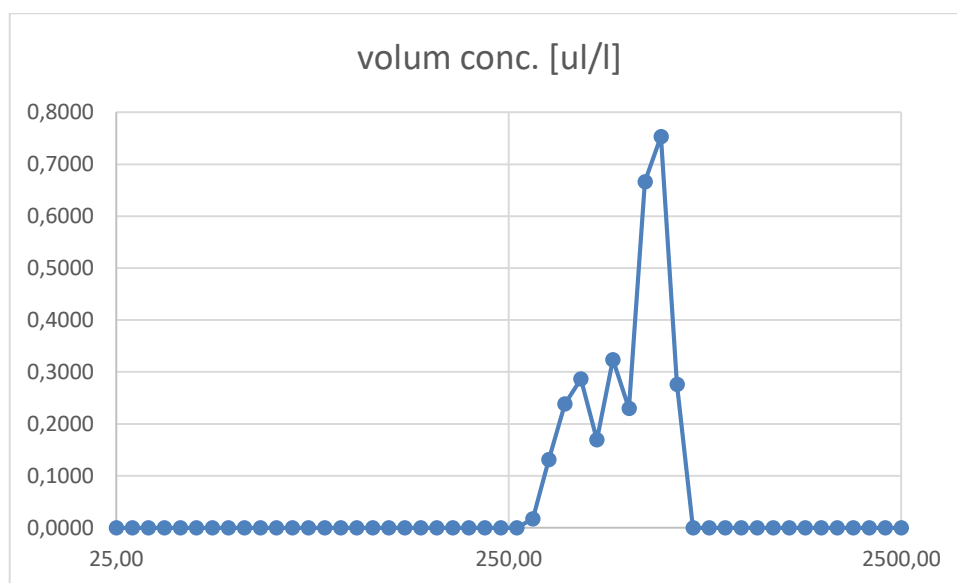


Figure 41: MPs volume distribution in Klimno Krk (Rijeka).

### 2.3.3 Split field campaign – October 2021 (Split area)

Table 20: CTD data recorded by OBU system from the boat in Split.

DATE	TIME	LAT	LON	TW[°C]	CW[mS/cm]	SW[ppt]
29/10/21	08:48:51	43.48595	16.48600	19.00	53.00	34.90
29/10/21	08:48:54	43.48595	16.48600	19.00	53.00	34.90
29/10/21	08:48:57	43.48595	16.48600	19.00	53.00	34.90
29/10/21	08:49:00	43.48595	16.48600	19.00	53.00	34.90
29/10/21	08:49:03	43.48595	16.48600	19.00	53.00	34.90
29/10/21	08:49:06	43.48595	16.48600	19.00	53.00	34.90
29/10/21	08:49:09	43.48595	16.48600	19.00	53.00	34.90
29/10/21	08:49:12	43.48595	16.48600	19.00	53.00	34.90

Table 21: Information related to the holo-sensor recording in Split (1 transect).

Mission Name	SPLIT 1
Location	Split (HR)
Time Begin	29/10/2021 09:52
Duration	00:47:07
Path Length	1.7km
Average speed	2.2km/h
Holograms collected at 20fps	49447
Holograms with particles	235

<i>Particles Detected</i>	298
<i>Particles that are clearly biota or fish eggs</i>	28
<i>Linear concentration [Particles/km]</i>	123 particles/km
<i>Volume concentration [Vol Particles / Vol Processed]</i>	9.051 ul/l

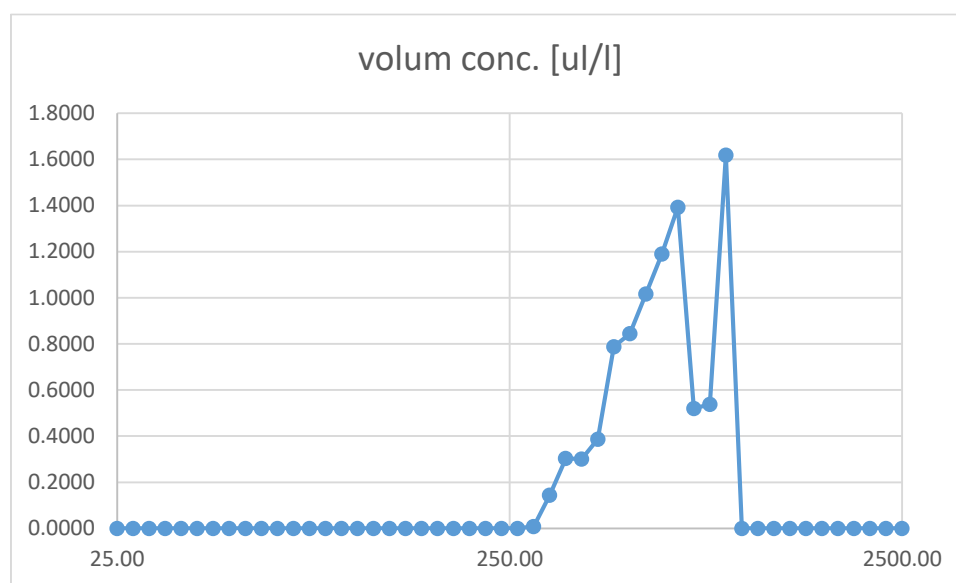


Figure 42: MPs volume distribution in Split (I transect)

Table 22: Information related to the holo-sensor recording in Split (II transect).

<i>Mission Name</i>	SPLIT 2
<i>Location</i>	Split (HR)
<i>Time Begin</i>	29/10/2021 10:48
<i>Duration</i>	00:52:16
<i>Path Length</i>	3.6km
<i>Average speed</i>	4.2km/h
<i>Holograms collected at 20fps</i>	46063
<i>Holograms with particles</i>	196
<i>Particles Detected</i>	229
<i>Particles that are clearly plankton or fish eggs</i>	95
<i>Linear concentration [Particles/km]</i>	33 particles/km
<i>Volume concentration [Vol Particles / Vol Processed]</i>	5.79ul/l

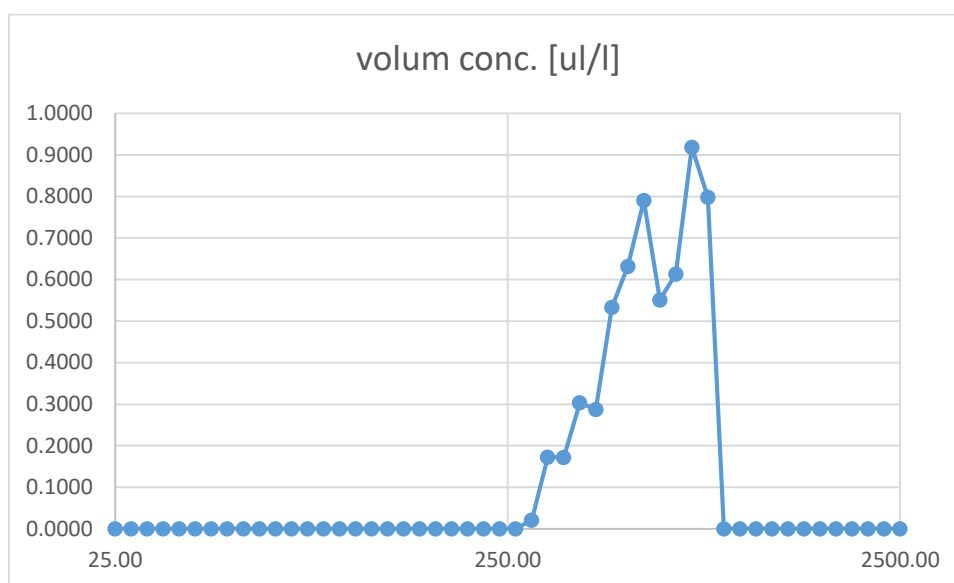


Figure 43: MPs volume distribution in Split (II transect)

### 2.3.4 Rijeka field campaign – May 2022 (Rijeka area)

Table 23: CTD data recorded by OBU system from the boat in Rijeka.

Date	Time	Conductivity[mS/cm]	Temperature[° C]	Depth[m]	Salinity[PSU]
04/05/2022	10:09:04	47.4064	15.77	0.25	38.37
04/05/2022	10:09:05	47.4013	15.78	0.25	38.36
04/05/2022	10:09:06	47.3445	15.77	0.25	38.31
04/05/2022	10:09:07	47.3489	15.77	0.24	38.32
04/05/2022	10:09:08	47.3581	15.76	0.24	38.34
04/05/2022	10:09:09	47.3723	15.76	0.26	38.35
04/05/2022	10:09:10	47.3782	15.76	0.25	38.36

Table 24: CTD data recorded by OBU system from the boat in Rijeka.

Date	Time	Temp.[°C]	Diss. O2 conc. [umol/l]	Turbidity [NTU]	Diss. O2_saturation[%]
04/05/2022	10:13:35	15.37	250.633	12.393	99.365
04/05/2022	10:13:40	15.52	250.012	12.879	99.421
04/05/2022	10:13:45	15.65	248.300	12.850	98.976
04/05/2022	10:13:50	15.64	249.795	12.983	99.569
04/05/2022	10:13:55	15.55	249.728	12.917	99.366
04/05/2022	10:14:00	15.53	250.464	12.927	99.612
04/05/2022	10:14:05	15.57	250.292	12.835	99.630
04/05/2022	10:14:10	15.58	249.328	12.879	99.253
04/05/2022	10:14:15	15.57	249.096	12.863	99.138

### 2.3.5 Goro field campaign – May 2022 (Po Delta)

Table 25: CTD data recorded by OBU system from the boat in Goro

Date	Time	Conductivity[mS/cm]	Temperature[°C]	Depth[m]	Salinity[PSU]
12/05/2022	08:46:30	45.48	19.66	0.18	33.28
12/05/2022	08:46:31	45.48	19.66	0.21	33.28
12/05/2022	08:46:32	45.48	19.65	0.19	33.28
12/05/2022	08:46:33	45.48	19.65	0.18	33.28
12/05/2022	08:46:34	45.47	19.65	0.19	33.28
12/05/2022	08:46:35	45.46	19.65	0.20	33.27
12/05/2022	08:46:36	45.46	19.66	0.18	33.26
12/05/2022	08:46:37	45.46	19.66	0.19	33.27
12/05/2022	08:46:38	45.45	19.66	0.16	33.26
12/05/2022	08:46:39	45.45	19.66	0.18	33.26

Table 26: CTD data recorded by OBU system from the boat in Goro

Date	Time	Temp.[°C]	Diss. O2 conc. [umol/l]	Turbidity [NTU]	Diss. O2_saturation[%]
12/05/2022	08:46:00	19.59	212.32	9.19	91.27
12/05/2022	08:46:05	19.59	213.49	16.94	91.77
12/05/2022	08:46:10	19.54	214.44	12.13	92.10
12/05/2022	08:46:15	19.55	214.51	11.56	92.14
12/05/2022	08:46:20	19.55	214.37	10.94	92.07
12/05/2022	08:46:25	19.46	214.10	10.40	91.81
12/05/2022	08:46:30	19.39	214.66	12.73	91.93
12/05/2022	08:46:35	19.59	214.66	68.86	92.27
12/05/2022	08:46:40	19.60	214.65	133.71	92.29

## 2.4 Aerial Drone Imagery

The University of Ferrara (LP-UNIFE) applied the innovative technology of an aerial drone to monitor the presence of macroplastic in the Po Delta site.

Unmanned aerial vehicles (UAVs), in fact, can provide a flexible platform for carrying compact digital cameras to acquire pictures of the coastal environment (Andriolo et al., 2020, Lo et al., 2020). A quick remote method can hence be represented by the use of UAVs equipped with instruments able to detect the AMD. Images collected during UAV missions can thus be used for identification, even in real time. The level of detail in detecting the AMD is related to the ground sample distance (GSD), which depends on the characteristics of the camera used for acquiring pictures and on the flight altitude of the drone.

UAV-based images have been used to describe dune morphodynamics (Andriolo et al., 2020, Fairley et al., 2020), including cases of small formations (Taddia et al., 2017, Taddia et al., 2021) in the coastal environment, and therefore represent an innovative, efficient, and cost-effective tool for litter mapping (Andriolo et al., 2021, Merlino et al., 2020). Moreover, the use of drones with an onboard real-time kinematic (RTK) global navigation satellite system (GNSS) receiver reduces, or even eliminates, the need for deploying ground control points (GCPs) during the acquisition of images in order to achieve a final centimeter-level accuracy (Taddia et al., 2020, Forlani et al., 2018) in positioning AMD items (Taddia et al., 2021).

As part of the NET4mPLASTIC project, some coastal areas have been detected by aerial photogrammetry through the use of a multi-rotor drone Phantom 4 RTK (*Figure 44*) equipped with a high resolution camera (20MPixel, f/2.8, 84 FOV-field of view).



*Figure 44: Phantom RTK aerial drone and joystick.*



### 2.4.1 Drone images data acquisition and elaboration

Separate automatic missions of the aircraft at a maximum altitude of 25 and 50 metres have been programmed for different surveys. During each flight, the drone, under the control of operators recognized by the National Civil Aviation Authority, took photographs ensuring an overlap between a frame and the other equal to 80% longitudinally and 60% transversely. The camera parameters (ISO and shutter speed) have been adjusted from time to time in relation to light conditions.

The survey campaigns that have been realized during the first two years of the NET4mPLASTIC Project are listed in the following table.

Table 27: Description of the main aerial drone surveys.

Site	Date	Flying Height		Orthophoto		DEM	
		25m	50m	25m	50m	25m	75m
Goro	26/06/2019	X	X	X	X		
Boccasette	09/11/2019	X	X	X	X		
Boccasette	14/11/2019	X		X			
Boccasette	06/12/2019	X		X			
Boccasette	17/02/2020	X		X			
Boccasette	25/06/2020	X	X	X	X		X
Boccasette	06/10/2020	X	X	X	X	X	X
Volano	05/11/2020	X			X		
Rosolina	10/11/2020	X	X	X	X		

In order to scale and georeference the photogrammetric models, the plano-altimetric coordinates of some photographic support points (PFA), clearly identifiable points in the frames were detected using the GNSS technique (Global Navigation Satellite System). These points have been materialized with appropriate panels positioned (Figure 45) and detected by the dual-frequency geodetic receiver, previously described, used in static-mode rapid connection to the permanent station above the operational headquarters of the offices of the former Province of Ferrara. This technique guarantees a precision of centimetric positioning and framing in the same reference system used for mouse-bathymetric surveys.

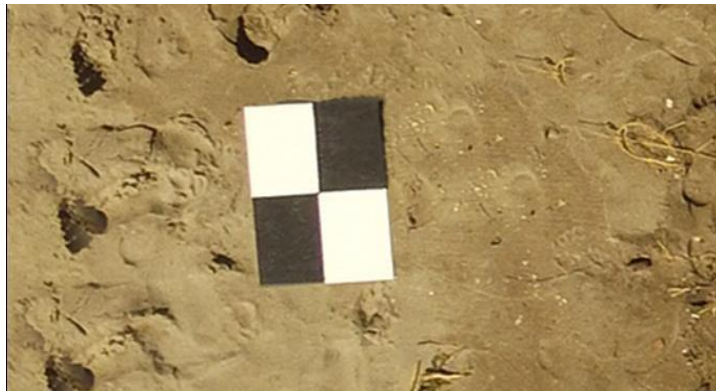


*Figure 45: Example of a target positioned on the ground.*

The ellipsoidal dimensions were then transformed into orthometrics through the use of the Convergo software. The uncertainty of the positioning of the targets by means of GNSS receiver used in N-RTK mode is equal to about 2 cm in plan and 4 cm in altitude.

The drone images were processed with the Agisoft Metashape digital photogrammetry software based on SFM (Structure from Motion) algorithms that can reconstruct a three-dimensional geometry from sequences of two-dimensional images.

The processing consists of several steps. First, for each of the three areas detected, the alignment of the frames is performed. On each image works an algorithm of features detection that allows to identify remarkable points (homologous points) allowing the alignment of the frames. The output of this phase is the generation of the "scattered cloud of points". We then proceed with the process of identification of the targets in the images (collimation) and the insertion in the software of the relative coordinates previously detected in the reference system WGS84-UTM32N (EPSG:32632).

Once these points have been determined, it is possible to solve the equations of colinearities that act as a bridge between the image space (two-dimensional) and the real space (3D), putting in relation:

- position in the image space of the bonding point;
- calibration parameters of the camera;
- external camera parameters (pose and orientation);
- coordinates in the real space of the binding point.

The system of equations is solved within a step called bundle adjustment, where the solutions obtained are optimized. This operation allows to scale and georeference the digital models obtained for the three areas detected and to calculate the errors on the inserted markers (difference between inserted and estimated coordinates) as well as the overall error of the model.

Image matching algorithms allow to search for "pixel to pixel" matches within a pair of images and to assign to each pixel a relative value of depth. It is therefore possible to generate a "dense cloud" representing the morphology of the detected area.

Then the points of the dense cloud become vertices of a triangle and all the triangles form a three-dimensional mesh (mesh) of the entire detected area. To create a realistic three-dimensional model, the mesh is then covered by the software with the graphic texture obtained from the photographs taken.

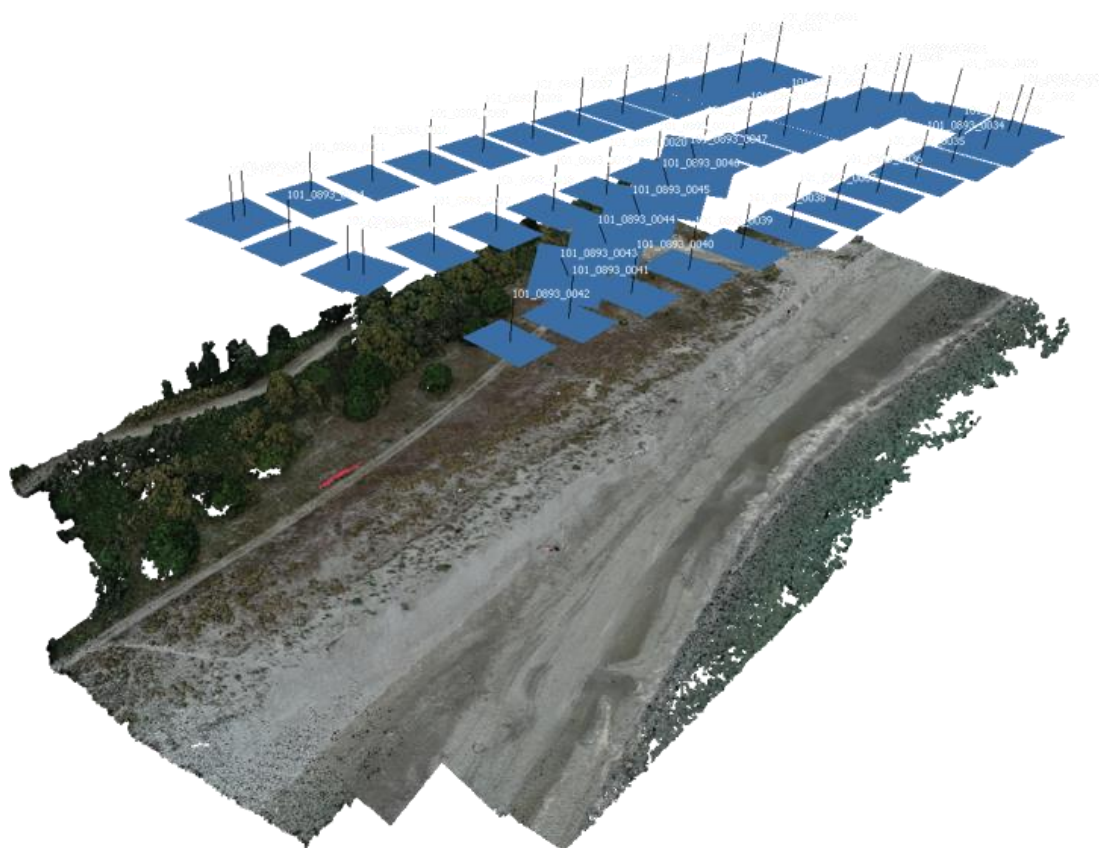


*Figure 46: Drone images acquisition and elaboration.*

From this model it was possible to obtain, for each of the three areas detected, an orthophoto that is an orthographic projection of the photogrammetric model on the cartographic plane. This projection is free of perspective deformation and has a metric value. Given the method used, the orthophoto obtained is characterized by remarkable precision, evaluable in the order of about ten centimetres that is compatible with the error of graphics and with the nature of the object of the relief.

To exclude non-soil vegetated areas from the 3D model, a specific filter is applied, using a classification algorithm able to distinguish them from the soil in a semi-automatic way. The automatic classification procedure consists of two steps. The first step predicts that the dense cloud is divided into cells of a certain size (in the relief in question was adopted a mesh 5x5 m). In each cell the lowest point is detected and classified as belonging to the soil. The triangulation of these points provides the first approximation of the soil model. In the second phase, all other points are classified by analysing their distance and slope from points classified as "*terrain*". The threshold values for distances and gradients must be specified: in this case the values adopted are 0.15 meters and 5 inches.

After the application of the filter, a manual classification phase was carried out based on the combined analysis of the elevation trend of the soil and the chromatic data (in order to exclude as far as

possible points that are not belonging to the ground from the subsequent processing steps). In the removed areas the model is reconstructed by interpolation. It is important to note that, in presence of dense vegetation, it is not possible to get the shares of the soil, and the model obtained can present some errors.

Subsequently, a DTM (digital terrain model) can be obtained from the 3D model, resuming in a digital model of the shares of the points belonging to the ground able to represent the morphology of the detected area. The DTM should be released as a raster image with varying dimensions' pixels, in relation to flight altitude (Geographical Information System - GIS software allows to query every single pixel to know its associated dimension).

Since photogrammetric techniques are based on the recognition of homologous points in the various frames, shiny, transparent or perfectly homogeneous surfaces, as a body of water (sea), are therefore not detectable. For this reason, and with the noise caused by the presence of waves, it was not possible to complete the photos mosaic phase on the portion of submerged seabed.



Figure 47: Example of drone imaging elaboration: orthophoto of Boccasette (flying height 50m).

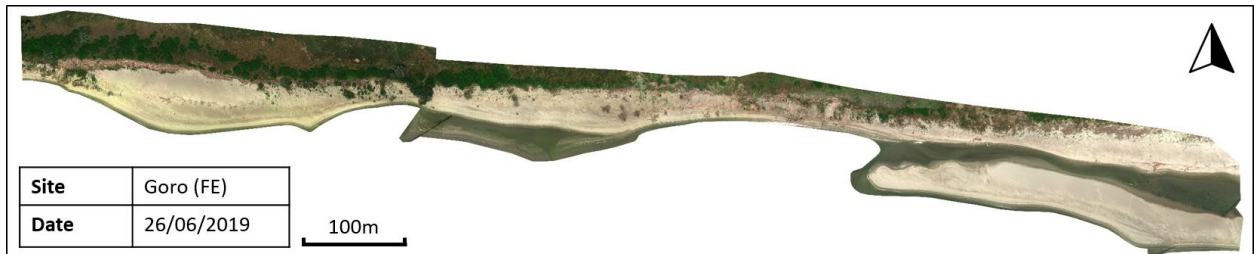


Figure 48: Example of drone imaging elaboration: orthophoto of Goro (flying height 50m).



Figure 49: Example of drone imaging elaboration: orthophoto of Rosolina (flying height 25m).

## 2.4.2 GIS elaboration and statistical analyses

In the context of this Project, the Department of Engineering of the University of Ferrara collaborated with the Department of Earth Science in order to acquire aerial drone images for the detection of macrolitter on the Natura 2000 site of Sacca di Goro—Foce del Po di Volano. At the same time a macro litter field campaign has been performed in order to compare and verify the items classification. A dedicated paper has been published within the Project (Taddia et al., 2021), and below are reported the main information on the activities of mapping and litter classification.

Orthomosaics generated using different ground resolution datasets were used to recognize the presence of litter items on the beach, together with NIR–NDVI data and DSM. All the marine litter collected contextually on the beach was analysed in the laboratory to identify and classify each item

according to the Master List of Categories of Litter Items (see D.4.1.1 for the methodology, D.4.2.2 for the main results).

To better understand the way expertise might influence accuracy with identification, operators with varying levels of experience in recognizing marine litter items from aerial drone pictures have been selected. Expertise in marine debris research and identification proved an important difference in determining operator accuracy. Assigning a level of confidence to the classification of items proved to be a crucial aspect in monitoring the degree of mapping accuracy. In fact, less confident classifications were often preferred by mapping operators due to the difficulty in distinguishing marine litter items from the background texture and recognizing it properly.

Larger items such as plastic bottles proved easy to identify on the orthomosaic and the DSM. This is because they cover a large number of pixels, and they also deviate considerably from the terrain topography. White pieces of plastic (e.g., polystyrene) can be distinguished both using the orthomosaic and multispectral information (i.e., NDVI).

However, recognizing them on the marine litter items may be difficult due to their small size and more rounded shape. Stoppers or bottle caps can be distinguished due to their circular shape, but the actual size results in the difference for success in recognizing them. Moreover, the visible side of the stopper is important. In fact, the accumulation of sand accumulated within the stopper can negatively affect the identification process. Flat objects, such as small pieces of plastics, are difficult to distinguish; their color may help in recognizing them on the orthomosaic, though such colors often fade over time and with exposure to the natural elements. Finally, transparent items (e.g., films, bags) are really hard to identify using all of the information acquired. They are often flat, transparent, and can also be partially covered by the sand, all of which make them less distinguishable.

Conversely, recognizing very small items is a very hard task: the spatial resolution on the ground should be increased, but generally this requires flying lower, limiting the extent of any flight mission. While microplastics do not contribute significantly to the total amount of marine litter items in terms of weight, they are an important component of the plastic pollution problem. The value of this approach is based on the mapping and quantification of larger items, representing a solution for a quick mapping of beached items (Taddia et al., 2021) (*Figure 50*).

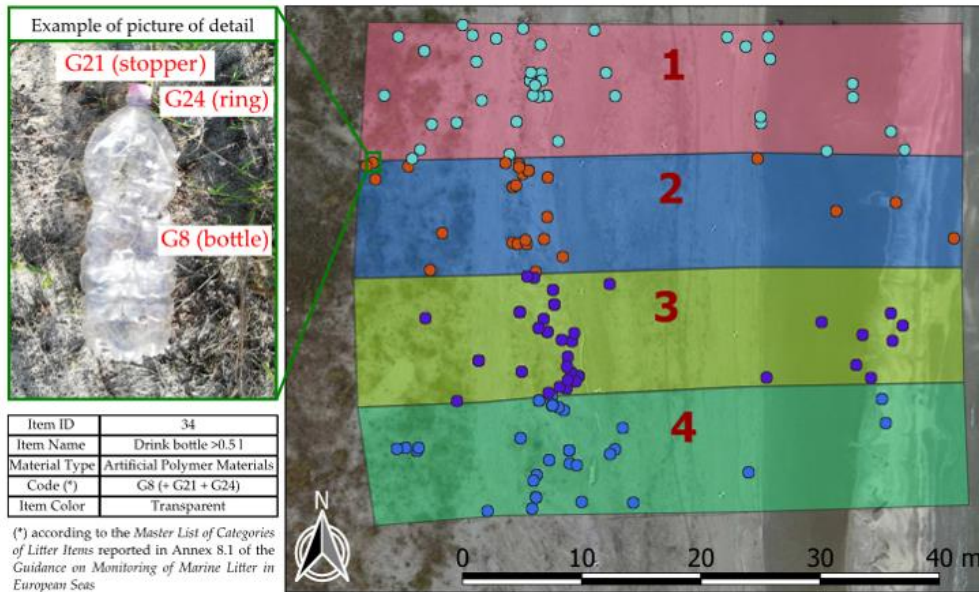


Figure 50: Marine litter mapping from aerial drone images (from Taddia et al., 2021)

The elaboration of the aerial drone images allowed also the production of specific maps, importing orthophoto and DEM images in GIS (Geographical Information System) environment, and using them for statistical analysis on the identification and categorization of marine litter items, and the linked relation with geomorphological facies and the presence of vegetation. A scientific paper on this topic has been submitted and other elaborations are in progress. In Figure 51 is shown an example of specific item (buoys) mapped on DTM image.

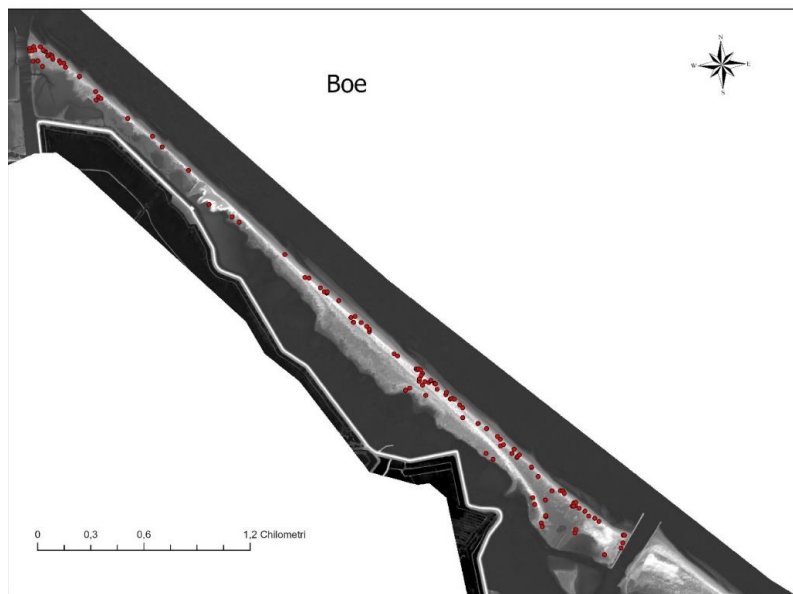


Figure 51: Example of drone imaging analyses: buoys identification on DTM map of Boccasette.



### 3 References

Andriolo, U.; Gonçalves, G.; Rangel-Buitrago, N.; Paterni, M.; Bessa, F.; Gonçalves, L.M.; Sobral, P.; Bini, M.; Duarte, D.; Fontán-Bouzas, A.; et al. Drones for litter mapping: An inter-operator concordance test in marking beached items on aerial images. *Mar. Pollut. Bull.* 2021, 169, 112542.

Andriolo, U.; Gonçalves, G.; Sobral, P.; Fontán-Bouzas, A.; Bessa, F. Beach-dune morphodynamics and marine macro-litter abundance: An integrated approach with Unmanned Aerial System. *Sci. Total Environ.* 2020, 749, 141474.

Fairley, I.; Horrillo-Caraballo, J.; Masters, I.; Karunarathna, H.; Reeve, D.E. Spatial Variation in Coastal Dune Evolution in a High Tidal Range Environment. *Remote Sens.* 2020, 12, 3689.

Forlani, G.; Dall'Asta, E.; Diotri, F.; Cella, U.M.D.; Roncella, R.; Santise, M. Quality Assessment of DSMs Produced from UAV Flights Georeferenced with On-Board RTK Positioning. *Remote Sens.* 2018, 10, 311.

Lo, H.S.; Wong, L.C.; Kwok, S.H.; Lee, Y.K.; Po, B.H.K.; Wong, C.Y.; Tam, N.F.Y.; Cheung, S.G. Field test of beach litter assessment by commercial aerial drone. *Mar. Pollut. Bull.* 2020, 151, 110823.

Merlino, S.; Paterni, M.; Berton, A.; Massetti, L. Unmanned Aerial Vehicles for Debris Survey in Coastal Areas: Long-Term Monitoring Programme to Study Spatial and Temporal Accumulation of the Dynamics of Beached Marine Litter. *Remote Sens.* 2020, 12, 1260.

Kvesić, M.; Vojković, M.; Kekez, T.; Maravić, A.; Andričević, R. Spatial and Temporal Vertical Distribution of Chlorophyll in Relation to Submarine Wastewater Effluent Discharges. *Water* 2021, 13, 2016. <https://doi.org/10.3390/w13152016>

Taddia Y., Corbau C., Buoninsegni J., Simeoni U., Pellegrinelli A. UAV Approach for Detecting Plastic Marine Debris on the Beach: A Case Study in the Po River Delta (Italy). *Drones.* 2021; 5 (4):140.

Taddia, Y.; Corbau, C.; Zambello, E.; Russo, V.; Simeoni, U.; Russo, P.; Pellegrinelli, A. UAVs to Assess the Evolution of Embryo Dunes. *Int. Arch. Photogramm. Remote Sens. Spat. Inf. Sci.* 2017, XLII-2/W6, 363–369.

Taddia, Y.; Pellegrinelli, A.; Corbau, C.; Franchi, G.; Staver, L.W.; Stevenson, J.C.; Nardin, W. High-Resolution Monitoring of Tidal Systems Using UAV: A Case Study on Poplar Island, MD (USA). *Remote Sens.* 2021, 13, 1364.

Taddia, Y.; Stecchi, F.; Pellegrinelli, A. Coastal Mapping Using DJI Phantom 4 RTK in Post-Processing Kinematic Mode. *Drones* 2020, 4, 9.